SANDIA REPORT
SAND2023-09532
Printed September, 2023

Sandia
National
Laboratories

Thermogravimetric Analysis (TGA) for Carbon Fiber and Glass Fiber Epoxy Composites and their Constituents

Raquel S.P. Hakes Weston-Dawkes, Brent C. Houchens, Sarah N. Scott

Prepared by
Sandia National Laboratories
Albuquerque, New Mexico 87185
Livermore, California 94550

Issued by Sandia National Laboratories, operated for the United States Department of Energy by National Technology & Engineering Solutions of Sandia, LLC.

Available to DOE and DOE contractors from

U.S. Department of Energy
Office of Scientific and Technical Information
P.O. Box 62
Oak Ridge, TN 37831

Telephone: (865) 576-8401
Facsimile: (865) 576-5728
E-Mail: reports@osti.gov
Online ordering: http://www.osti.gov/scitech

Available to the public from

U.S. Department of Commerce
National Technical Information Service
5301 Shawnee Road
Alexandria, VA 22312

Telephone: (800) 553-6847
Facsimile: (703) 605-6900
E-Mail: orders@ntis.gov
Online order: https://classic.ntis.gov/help/order-methods

ABSTRACT

In this work, thermogravimetric analysis (TGA) was performed on samples of a carbon fiber epoxy composite, a glass fiber epoxy composite, and a mixed carbon fiber/glass fiber epoxy composite, as well on each constituent material (polymer epoxy, carbon fibers and glass fibers). TGA was conducted for heating rates from 1-20 C/min with purified purge gases of nitrogen and dry air.

For the fiberglass composite, we find that ~70% of the material remains after heating in air to 1200 C. For the carbon fiber epoxy composite, we observe greater mass loss as the carbon fibers can oxidize, leaving little material by the end of the test. The mixed composite, which has a 2:1 ratio of glass fibers to carbon fibers, experienced a total mass loss between the two other composites. By determining the relationship between the thermal decomposition of a composite material and its constituent materials, we can predict the fire behavior of novel composites during the material design phase.

The raw data from these experiments can be found at: https://cee-gitlab.sandia.gov/omd/experimental-data/-/tree/master/tga

ACKNOWLEDGMENT

The authors would like to thank several people including Brian McKay and Gustavo Nungaray, who assisted with procuring composite samples, and Adriana Pavia-Sanders and Karla Reyes for guidance and expertise with TGA instrumentation.

Thanks to Matthew Kury for reviewing this report and providing valuable feedback.

CONTENTS

LIST OF FIGURES

LIST OF TABLES

NOMENCLATURE

Abbreviation	Definition
CF	Carbon fiber
CFE	Carbon fiber epoxy composite
CFGFE	Combined carbon fiber, glass fiber epoxy composite
GF	Glass fiber
GFE	Glass fiber epoxy composite
TGA	Thermogravimetric Analysis

1. INTRODUCTION

Fiber reinforced plastics are an attractive engineering material due to their low weight-to-strength ratio. They have been extensively used in automotive and aeronautical industries, as well as other industries where a light weight, yet strong, material is advantageous. However, unlike more traditional engineering materials such as metals, fiber reinforced plastics can be a source of fuel in a fire. At temperatures as low as 250°C, epoxies can start to pyrolyze, generating flammable gases. In order to understand the safety risks associated with these materials, it is necessary to understand their behavior when exposed to temperatures above their intended use.

Researchers have been studying fiber reinforced plastics for the past five decades. In the 1970s and 1980s, researchers were first understanding the mechanical effects of the structure of the composite, for example, how using woven fabrics compared to using chopped fibers [1, 2]. Experimental programs attempted to answer questions revolving around the minimum flux for ignition and the extinction characteristics of these new materials [3], as well as how they would perform under high heat fluxes [4]. One-dimensional models were created to understand thermal [5, 6] and thermo-mechanical [7] responses of composites when exposed to heat sources. These models required a range of material properties to be measured [8, 9], particularly those characterizing the thermal decomposition of the material [10, 11].

While this early research began to answer fundamental questions about the fire safety of fiber reinforced plastics, the number of these types of materials has increased exponentially in the intervening years. Simultaneously, experimental and computational techniques have advanced in both capability and accuracy. Experimental programs have used the cone calorimeter to obtain the minimum heat flux for piloted ignition [12–14], investigated how different epoxy and fiber types effect ignition [15, 16], explored the effects of the thickness of the sample [17], and determined how the percentage of fibers to polymer affects flammability [18]. Other researchers have investigated how flame spread is affected by the presence of high conductivity directional fibers [19].

Central to the issues of flammability and integrity of the composite structure is the need to understand the decomposition mechanism for these materials. This typically includes using thermogravimetric analysis (TGA) to track mass loss versus temperature (at a specified heating rate) and differential scanning calorimetry (DSC) to monitor heat flux versus temperature. TGA gives researchers insight into the reaction mechanism, while DSC gives information about the specific heat and heat of reaction.

TGA tests produce data relating the temperature, T, the time, t, and a measure of mass (e.g. mass, density, concentration) α. For a constant pressure, the loss $\frac{d\alpha}{dt}$ can be generally described by:

$$\frac{d\alpha}{dt} = k(T)f(\alpha) \tag{1.1}$$

where $k(T)$ can be represented by an Arrhenius rate:

$$k(T) = Aexp\left(\frac{-E}{RT}\right) \tag{1.2}$$

and where $f(\alpha)$ can take on many forms in solids, but for our purposes will take on the form:

$$f(\alpha) = (1-\alpha)^n \tag{1.3}$$

In addition, a reaction mechanism must be formed. The simplest of these mechanisms consist of one step, and increase in complexity from there. Generally, the form of the reaction is:

$$Reactants \longrightarrow \nu_s Products_{solid} + \nu_g Products_{gas} \tag{1.4}$$

where ν_s and ν_g are the fractions of solid and gas products, respectively. Other researcher have conducted TGA on composite materials. Quintiere *et al.* [12] conducted TGA tests on carbon fiber epoxy composites under inert conditions at heating rates of 1 to 30 C/min, up to 700 C. They determined a residue fraction of 0.74 at the end of the tests, for a composite that initially was 60% carbon fiber and 40% epoxy. Since the TGA was only done for inert condition, it is assumed that only the epoxy decomposed, and the mass remaining at the end of the test is a mixture of carbon fiber and char developed during the reaction.

Dodd *et al.* [22] conducted TGA tests for carbon fiber epoxy composites for a range of heating rates (2 to 500 C/min up to 727 C) using samples with a 2-mm edge length, cut from a thin square sheet. As is true in the other literature data, there was a delay in the temperature at which the peak mass loss occurs as the heating rate increases. In addition, in the inert environment, the amount of char produced decreased as the heating rate increased, producing 18% to 24% char (by initial mass epoxy).

Tranchard *et al.* [23] collected data for TGA under air and nitrogen environments, for a heating rate of 20 C/min up to 1500 C using thin square samples. Under nitrogen conditions, Tranchard *et al.* observed that 26% of the mass was lost (for a composite that was 35% epoxy, 55% carbon fiber), and that char residue had formed. As they knew the exact composition of their composite (which is not always possible due to proprietary blends), they were able to attribute the 9% by weight char residue to the decomposition of uncrosslinked hardener (4,4′-Diaminodiphenyl sulfone), polyesthersulfone, and epoxies. From the TGA preformed in air, they conclude that, in addition to oxidizing the carbon fibers, oxygen promotes the formation of the transient char species. In addition, from Fourier transformed infrared spectroscopy (FTIR), they found that the main gas products evolved were H_2O, the decomposition products of PA6, phenol, CH_4, COS and CO.

As part of a larger study investigating the impact of geometry on the flammability of composites, Fateh *et al.* [17] performed TGA and FTIR on samples that were ground into a powder, and heated to 800 C at rates of 5, 10, and 20 C/min. TGA was only run under nitrogen purge gas conditions. For a sample that was 30% epoxy by mass initially, between 20 and 25% of the mass was lost at the end of the test. The amount of char remaining increased with heating rate, which is the opposite result of Dodd *et al.*, Quintiere *et al.*, and Tranchard *et al.* In addition, Fateh *et al.* observed less char production than other researchers. However, unlike Dodd *et al.* and Tranchard *et al.*, Fateh *et al.* used ground samples for TGA (Quintiere *et al.* does not state the sample preparation). This may have had an effect on the char production.

While much of the work relating to the fire safety of carbon fiber epoxy composites has focused on the decomposition of the epoxy, the carbon fibers can also oxidize at sufficiently high temperatures (600-1000 C). Branca *et al.* [25] found three main reaction for their composite: an oxidative decomposition of the resin, followed by an oxidation of the char produced by the former step, and finally an oxidation of the fibers.

In this work, we present TGA data for a both carbon fiber epoxy (CFE) and glass fiber epoxy (GFE), both impregnated with the same UF3362-100 epoxy resin and cured. Details of the prepreg materials are given in the appendix. The CFE and GFE was cured in sheets, cut into samples, and decomposed via TGA. Each of the constituents fibers were also subjected to TGA separately after chemically extracting them from their prepreg resin. During the cure under vacuum a small portion of epoxy "bleeds off" near the edges of the sheets. This cured epoxy bleedoff was also separately subjected to TGA. The samples were tested in both air and nitrogen environments at heating rate of 1, 5, 10, and 20 [C/min]. A subset of the samples contained both carbon fiber and fiberglass, and it is theorized that by properly mixing the results from the constituent reactions, the mass loss curve of the mixture can be predicted.

In Chapter 2, we discuss the methods used to conduct the tests. In Chapter 3, the data for the each of the constituents (carbon fibers, glass fibers, epoxy) are presented, while in Chapter 4 the data for the composites is presented. In Chapter 5 we show a method for predicting the mass loss curve for mixed materials. Finally, Chapter 6 presents a summary and future work.

2. METHODS

2.1. Materials

Tests were conducted for three composite materials and their constituent components (i.e. the epoxy bleedoff and the fiber used to fabricate the composite). The constituents, shown in Figure 2-1, included two different fibers: carbon fiber and glass fiber. The same epoxy was used in all three composite materials (shown in Figure 2-1 and 2-2).

The composite materials are shown in Figure 2-3. All composite materials were approximately 33-34% epoxy, with slight variations between the specific composite. The composites include a carbon fiber epoxy composite, AS4C-UF3362 (fabric number SC561-8HS-3K, fiber type fill HexTow AS4 C GP 3K, resin UF 3362-100), a glass fiber epoxy composite (7781-UF3362, fabric number 7781-8HS-50, fiber tarn type fill ECDE 75 1/0, resin UF 3362-100), and a combined carbon and glass fiber epoxy composite, which had a ratio of 2:1 glass fiber to carbon fiber.

2.2. Thermogravimetric Analysis

For all the samples, we conducted thermogravimetric analysis (TGA) experiments which measure the mass of a sample versus temperature for a given heating rate. The samples were decomposed in 85 microliter (6.8-mm diameter) alumina crucibles (see 2-2), and those conducted in nitrogen where covered with a vented alumina lid (not shown). TGA is used to develop reaction mechanisms for the decomposition of a material and determine the kinetic parameters of each reaction.

TGA requires small samples, as the basic assumption is that the temperature of the sample is uniform throughout. Epoxy and composite samples were left whole, cut to ~3 mm in length. The height of each sample was dictated by the sheet of composite or epoxy. Fibers were also left whole and wrapped to fit into the crucibles. Although TGA samples are frequently ground, here the samples are left whole (for the composite experiments) with the same orientation as that of a larger part of interest, to replicate any effects of the layers in the composite.

Figure 2-1. From left to right: glass fibers, carbon fibers, cut sample of epoxy, all before decomposition.

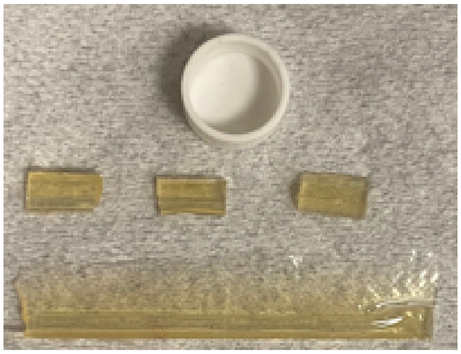

Figure 2-2. Top: crucible used in experiments. Middle: Cut pieces of epoxy bleedoff for experiments. Bottom: Epoxy bleedoff from the cure cycle of the composite fabrication. The bleedoff epoxy is uneven thickness; pieces used in experiments are cut from thick edge.

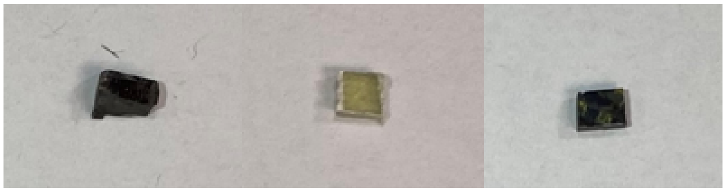

Figure 2-3. From left to right: carbon fiber epoxy composite, glass fiber epoxy composite, combined carbon fiber and glass fiber epoxy composite, all cut to sizes used in TGA experiments.

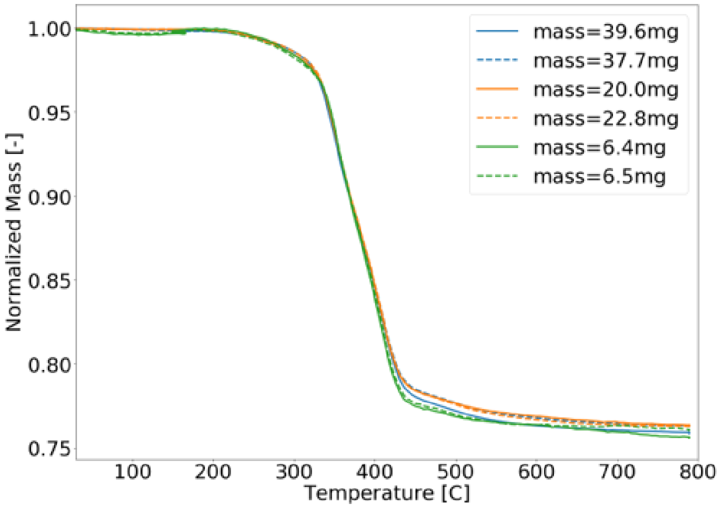

Figure 2-4. Mass loss as a function of temperature for carbon fiber epoxy composite in N_2 at a heating rate of 5 C/min shows negligible differences with sample sizes ranging from 6-40 mg.

2.2.1. Test Conditions

Test conditions explored changing materials, heating rates, and purge gases, as shown in Table 2-1. A total of 2-6 repetitions are available for the range of experiments conducted (a minimum of 3 repetitions were conducted for each main condition; however, issues with some measurements caused us to remove some clearly problematic data, e.g. mass readings below 0 mg).

Table 2-1. Experimental matrix of materials and heating rates tested for two purge gases.

Materials	Heating rates	Purge gas characteristics
CF, GF (N_2 only), epoxy, CFE, GFE, CFGFE	1, 5, 10, 20 C/min	N_2 (20 mL/min, with lid), dry air (40 mL/min, no lid)

First the influence of sample size, crucible configuration (open or closed by a lid), and gas flow rate was explored for a small subset of experiments to select conditions such that these effects could be neglected in subsequent testing. The impact of sample size on mass loss was investigated for three size ranges of samples (6-7 mg, 20-23 mg, and 37-40 mg) for CFE in N_2 at 5 C/min. As shown in Figure 2-4, there is no notable, consistent influence of sample size on the mass as a function of temperature.

All air tests were conducted with no lid on the crucible, to avoid a potentially limited supply of oxygen from influencing the decomposition behavior. For inert tests, the impact of using a lid versus no lid was investigated for the epoxy and all three composites at 20 C/min. Figure 2-5 shows

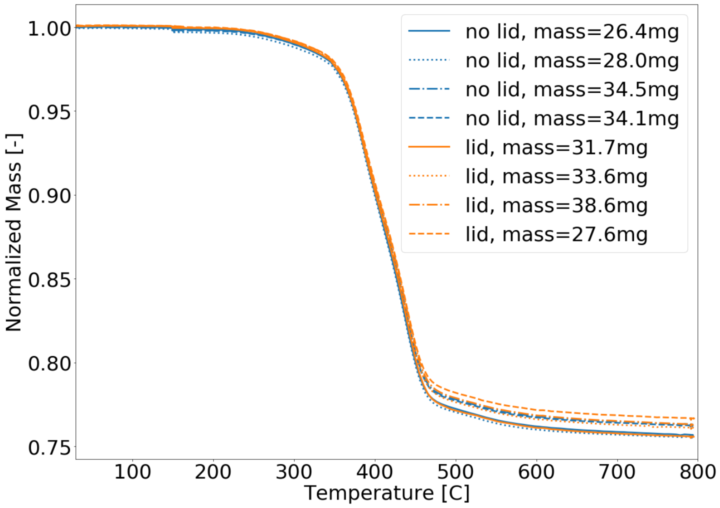

Figure 2-5. Mass loss as a function of temperature for CFGFE in N_2 at 20 C/min shows negligible impact of including a lid or not on the crucible.

the mass loss curve for CFGFE which exhibits no difference with or without a lid. The results shown here are representative of the other fuels tested. With no impact of a lid, all inert tests were conducted with a lid.

While all tests using N_2 as a purge gas used a flow rate of 20 mL/min, the impact of flow rate for air tests was investigated to ensure that a potentially limited oxygen supply would not influence test results. Figure 2-6 shows the impact of air flow rate on the mass loss of CFE at 20 C/min heating. The rate and temperature of the oxidation reactions (above approximately 500 C) are clearly influenced by flow rate, likely due to limited oxygen availability at the lower flow rates. This trend is more evident when investigating the derivative of the mass loss curve, shown in Figure 2-7. In particular, at the lowest flow rates, the two separate reactions in the range of 550-700 C do not appear. Similarly, the rate of reaction for the reaction taking place around 900 C increases as flow rate increases. At 30 mL/min and 40 mL/min, behavior begins to converge. As a result, all tests in air were conducted at 40 mL/min.

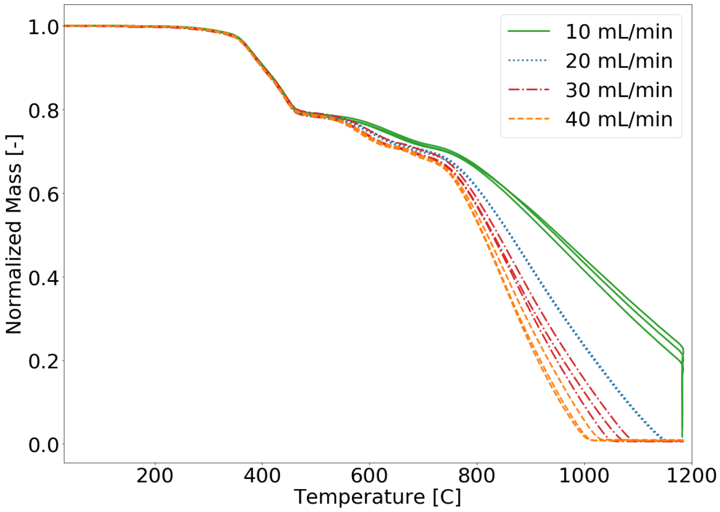

Figure 2-6. Mass loss as a function of temperature for carbon fiber epoxy composite in air for differing flow rates of air. For higher flow rates, oxidation reactions appear to occur at a faster rate, indicating the low flow rates are likely oxygen-limited. As the curves begin to collapse for 30 and 40 mL/min, we choose 40 L/min as a non-oxygen-limited flow rate for air.

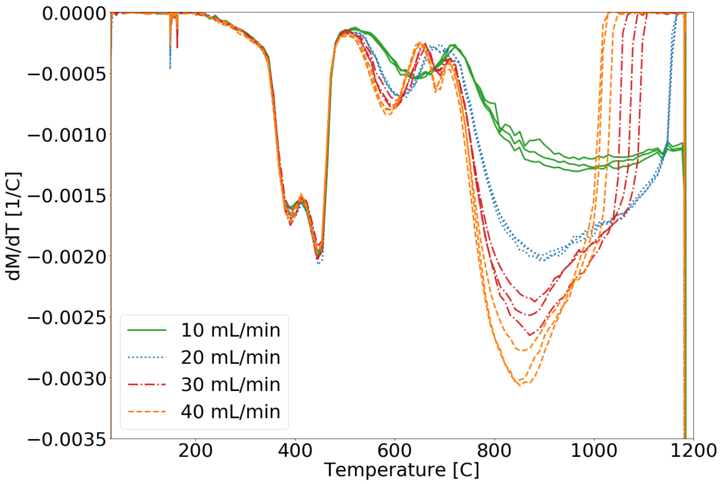

Figure 2-7. Derivative of the mass loss as a function of temperature of carbon fiber epoxy composite in air for differing flow rates of air. Similar to the mass loss plot, we see clearly that experiments conducted with air flowing at 10 or 20 mL/min miss the two reactions occurring between 600-800 C. Some differences in rate remain between 30 and 40 mL/min, but all reactions are captured.

3. CONSTITUENTS RESULTS

In this chapter, we present the TGA data for each of the constituent materials: epoxy, carbon fiber, and glass fiber. Each of these materials were tested in both air and nitrogen purge gas, at heating rates of 1, 5, 10, and 20 [C/min], as described in Chapter 2.

3.1. Epoxy

3.1.1. Epoxy in Nitrogen

In nitrogen, we expect the epoxy to decompose through the pyrolysis pathway. This will produce flammable gases, and leave behind a charred material. In Figure 3-1, we present the data for the epoxy in nitrogen at all heating rates. There are several things to note. First, approximately 75% of the material is lost in this decomposition process. What remained in the crucible was a small piece of charred material. The char was structurally stable, though it did beak apart more easily than the virgin epoxy. Next, as the heating rate increases, the reaction happens at a higher temperature (the shift of the data to the right). While 5, 10, and 20 C/min rates produce approximately the same amount of mass loss, the 1 C/min loses about 5% less mass. We theorize that slowing down the heating rate allows for the activation of different reaction pathways, which cause this difference.

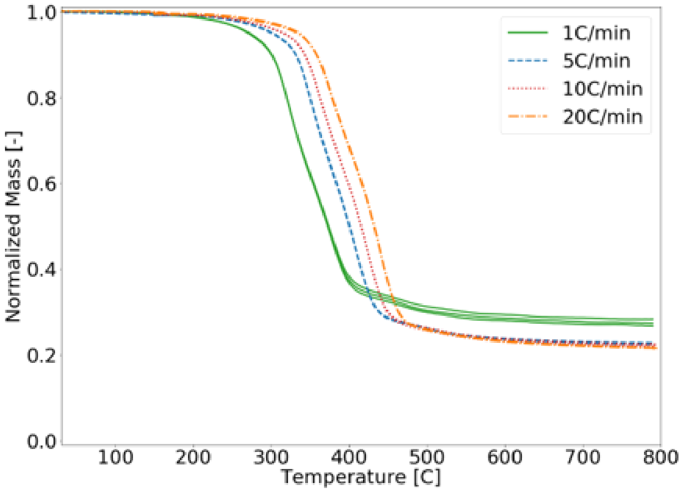

Figure 3-1. Normalized mass loss as a function of temperature for epoxy at four heating rates decomposing in N_2. All heating rates show relatively uniform behavior with consistent reaction rates, but reactions occur at slightly larger temperatures as the heating rate is increased. Notably, the 1 C/min heating rate has more remaining mass than the higher heating rates (three replicates of the 1 C/min heating rate experiment are shown).

3.1.2. Epoxy in Air

In air, we expect the epoxy to decompose through the pyrolysis pathway, as observed in nitrogen, but also to undergo an additional oxidizing reaction. Figure 3-2 shows the mass loss curve for the epoxy in air. We see a curve similar to that in nitrogen until approximately 425 C. At this point, the slope of the curve changes. We consider the mass loss before 425 C to be due to the pyrolysis reaction, and after to be the oxidation of the char. By the end of the test, there was very little material left in the crucibles. We again see that the 1 C/min tests behaves differently – the change in the slope occurs at a higher normalized mass than for the other heating rates. We also see for the oxidation period (mass loss after 500 C) we can see the slope changes with heating rate, where as the slope for the pyrolysis step does not change with heating rate. This may be due to mass and heat transfer effects. Since the oxidizing reaction is reliant on oxygen, higher heating rates may be experiencing oxygen limited decomposition.

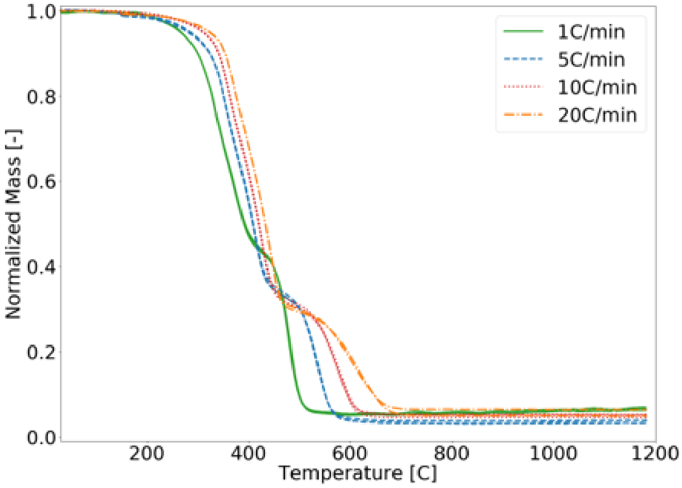

Figure 3-2. Normalized mass loss as a function of temperature for epoxy at four heating rates decomposing in air. Pyrolysis reactions below 400 C show similar behavior to that observed in N_2. Oxidation reactions occur at slower rates as the heating rate is increased (see slope of curve between 500-700 C). The remaining mass differs slightly between the four heating rates.

3.2. Fibers

3.2.1. Fibers in Nitrogen

In nitrogen, we expect to see no decomposition carbon fibers or fiberglass. Figure 3-3 shows no mass loss. Carbon fiber, while not inert, requires oxygen to decompose at these temperatures. Fiberglass, on the other hand, is not an organic material, and therefore is expected to never decompose, regardless of the presence of oxygen. At the end of the test, the carbon fiber and the fiberglass both looked similar to their appearance at the start of the test.

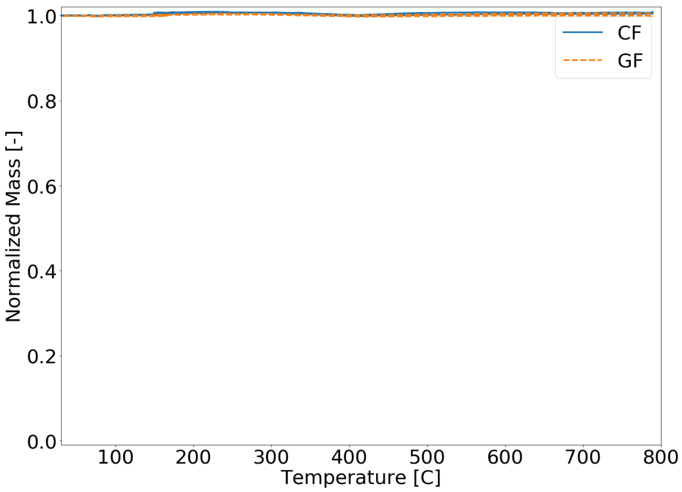

Figure 3-3. Normalized mass loss as a function of temperature at 5 C/min for both fibers, CF and GF, in N_2. As anticipated, neither fiber experiences decomposition in an inert environment.

3.2.2. Carbon Fiber in Air

In air, we expect the carbon fiber to oxidize as seen in Figure 3-4. As in the case with the epoxy, we note a pronounce difference between the heating rates. While the onset temperature increased with heating rate, the slope of the decomposition is similar for the 1, 5 and 10 C/m tests. However, for 20 C/min, the slope is slightly lower. Again, this may be due to a limiting of the mass transfer of oxygen.

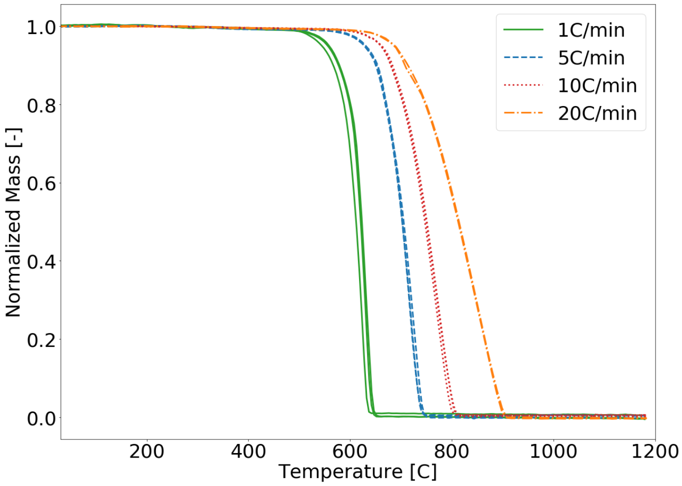

Figure 3-4. Normalized mass loss as a function of temperature for carbon in air, shown for all four heating rates. Oxidation occurs at higher temperatures for higher heating rates; however, the differences in reaction rate at different heating rates are less stark for carbon fiber as compared to epoxy. All heating rates completely consume the fibers.

4. COMPOSITE RESULTS

In this chapter, TGA experiments of cured composites which include both fibers (glass, carbon, or both) and epoxy are described.

4.1. Carbon Fiber Epoxy Composite

4.1.1. CFE in Nitrogen

In Chapter 3 we showed that epoxy pyrolyzes in nitrogen, while the carbon fibers undergo no reaction. Therefore, in nitrogen we expect the composite of the two materials to decompose to approximately the mass of the carbon fiber plus the mass of the char that is formed. As the mass fraction of epoxy is approximately 33%, and in the epoxy-only tests approximately 25% of the mass remained, we expect about 75% (67% plus 0.25 × 33%) of the mass should remain in composite CFE tests in nitrogen. Figure 4-1 shows approximately this expected behavior. As with the epoxy, we see that the onset for the reaction increases with heating rate, and that the 1 C/min has a higher residual mass than the other heating rates. However, we do now see some differentiation in the residual mass of the 5 and 10 C/min vs the 20 C/min. The presence of the carbon fiber may favor reactions that produce more char. At the end of the experiments, the samples where intact, however the layers of carbon fiber were easily separated with tweezers.

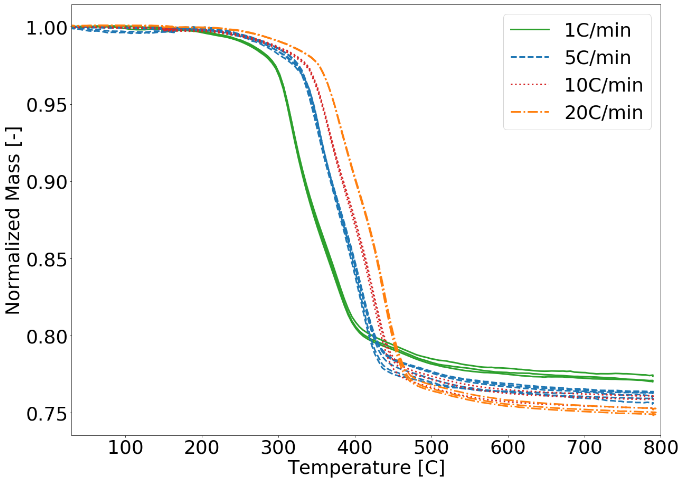

Figure 4-1. Normalized mass loss as a function of temperature for CFE at four heating rates decomposing in N_2, with replicates for each experiment. Similar to epoxy alone, reactions occur at slightly higher temperatures for higher heating rates, but share similar reaction rates. A notable difference is that remaining mass is more influenced by heating rate compared to epoxy alone. While the lowest heating rate still has distinctly more mass remaining (similar to epoxy), the mass remaining for higher heating rates is not similarly identical. In particular, tests conducted at 20 C/min consumes more mass than those at 5 or 10 C/min.

4.1.2. CFE in Air

Similar to the case in nitrogen, in air we see that the carbon fiber composite follows the trend of the constituents, shown in Figure 4-2. Here, we see four distinct changes in slope: 100-80% mass, 80-70% mass, 70-60% mass, and finally 60-0% mass. The first step is the pyrolysis of the epoxy, followed by the oxidation of the char. The next stage is likely a combination of the char and carbon fiber oxidizing. Once all the char has been consumed, the slope changes again as now only carbon fiber is oxidizing. As was the case with both the carbon fiber and the epoxy, we see a marked difference in mass loss for the oxidizing reactions as the heating rate increases. This is particularly evident in the third and fourth segments. For the 1 C/min heating rate, the transition between segments three and four occurs at a much lower mass than the other heating rates. This is likely due to the lower decomposition temperature of the carbon fiber at this heating rate. This extends the range of temperatures where both the char and the carbon fiber are decomposing. We also see a large change in the slope of the fourth segment as the heating rate increases. This is likely due to oxygen limitation. At the end of the tests, there was nothing left in the crucibles.

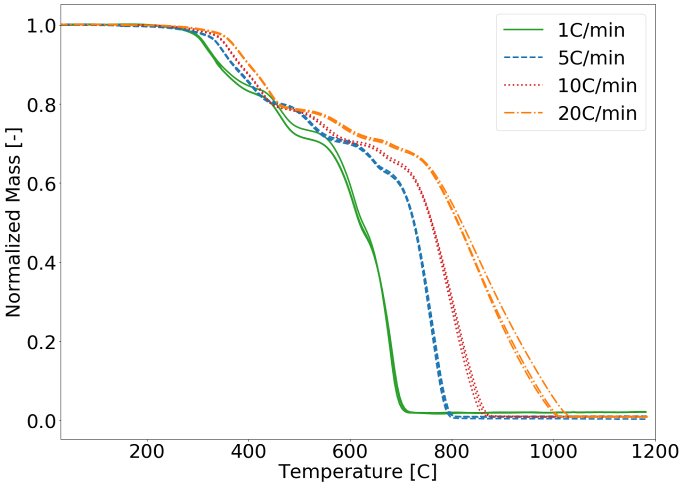

Figure 4-2. Normalized mass loss as a function of temperature for CFE at four heating rates decomposing in air, with replicates for each experiment. Trends are similar to the superposition of epoxy in air and carbon fiber in air. That is, pyrolysis reactions are fairly similar for different heating rates, while oxidation reactions occur at higher temperatures and slow rates for higher heating rates. This trend is particularly notable for the 20 C/min heating rate. Remaining mass is fairly constant for all heating rates except 1 C/min.

4.2. Glass Fiber Epoxy Composite

4.2.1. GFE in Nitrogen

As was the case with the carbon fiber composite, we see that the mass loss in nitrogen in governed by the pyrolysis of the epoxy (Figure 4-3). We see the same trends as before, where onset temperature of decomposition increases with heating rate, and the mass remaining decreases with heating rate. At the end of the test, the sample was still intact, but rather than white, it was now completely black (making it indistinguishable from the the carbon fiber epoxy samples). The layers of fiberglass could be easily pulled apart, as was the case with the carbon fiber composite.

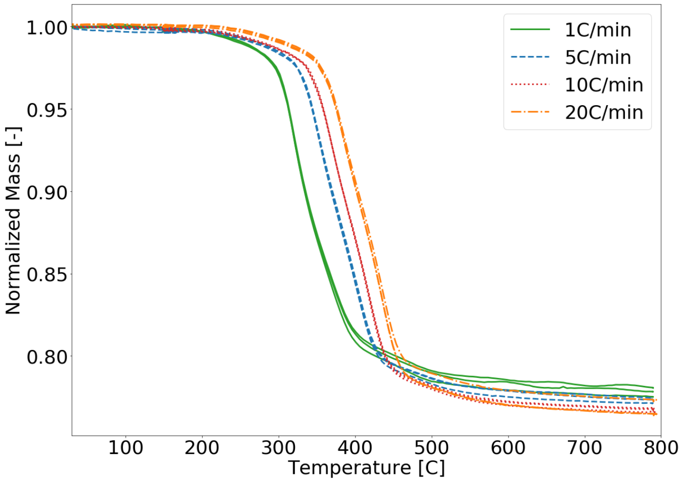

Figure 4-3. Normalized mass loss as a function of temperature for GFE at four heating rates decomposing in N_2. Trends with heating rate are analogous to those observed in CFE.

4.2.2. GFE in Air

Since the fiberglass is inert, including oxygen causes the char to oxidize, but still leaves approximately 70% of the mass behind (Figure 4-4). Here we can see two segments, the first corresponding to the pyrolysis reaction, and the second to the char oxidation. This curves appear similar to the epoxy in air (Figure 3-2). We again see the onset temperature increase with heating rate, and for the first time in air, we see a difference in the final mass that depends on heating rate. The presence of the inert glass may prevent the oxidation of some small amount of char, or possibly an oxide is being formed. At the end of the test, the fiberglass had melted, then re-solidified into a pool at the bottom of the crucible. This suggests the melting temperature of this fiberglass is between 900 C and 1200 C, as the fiberglass did not melt in the in the nitrogen purge gas tests to 800 C.

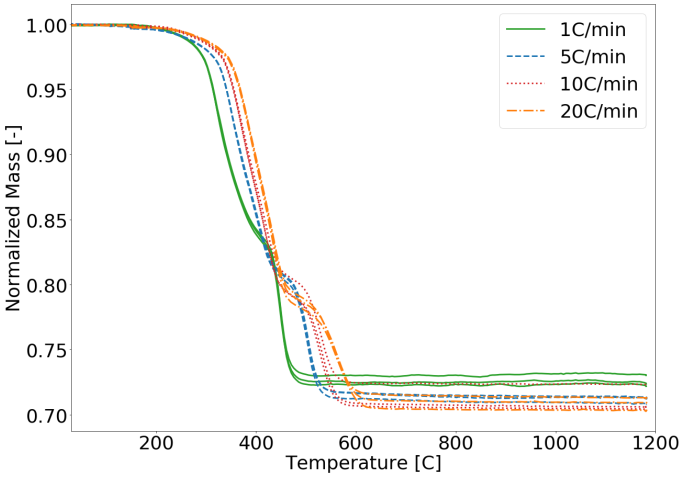

Figure 4-4. Normalized mass loss as a function of temperature for GFE at four heating rates decomposing in air. Pyrolysis reactions are fairly similar for different heating rates, while oxidation reactions occur at higher temperatures and slow rates for higher heating rates (shown in the reaction occurring between 500-600 C). Due to the inert nature of glass fiber, GFE has substantial remaining mass at the end of a test, and most decomposition has occurred by 600 C. The experiments at 1 C/min have notably more remaining mass than the other heating rates; however, trends in remaining mass with higher heating rates are not evident.

4.3. Combined Carbon Fiber-Glass Fiber Epoxy Composite

4.3.1. CFGFE in Nitrogen

In this mixed fiber composite, we see that the mass loss curve again looks like epoxy alone, with the final mass approximately equal to the mass fraction of the fibers (Figure 4-5). Since the fiberglass is inert, and the carbon fiber does not decompose without oxygen at these temperatures, this behavior is expected. We can again see the trend of the onset temperature increasing with heating rate, and the final mass loss decreasing in with heating rate. At the end of the test, the sample was intact, though the layers had delaminated. Char covered all the layers, making the fiberglass and carbon fiber layers visually indistinguishable.

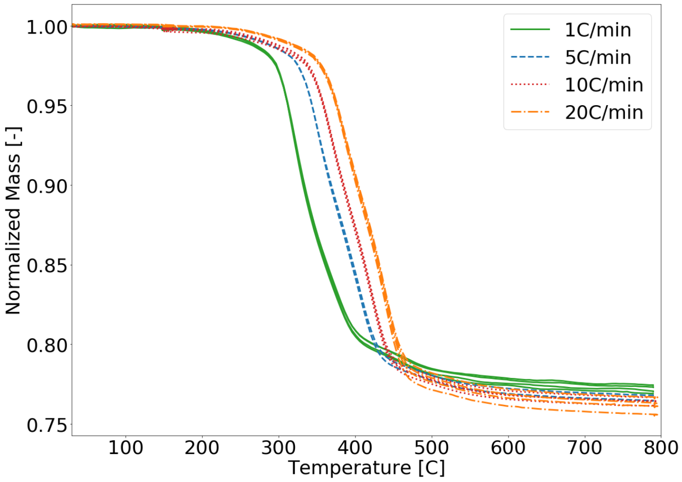

Figure 4-5. Normalized mass loss as a function of temperature for CFGFE at four heating rates decomposing in N_2. Trends with heating rate are analogous to those observed in CFE.

4.3.2. CFGFE in Air

In air, the mixed composite has a final mass fraction that is approximately equal to the mass fraction of glass fiber in the sample (Figure 4-6). We can see the three slope changes, associated with the pyrolysis of the epoxy, the oxidation of the char, and the oxidation of the carbon fiber. We can see the change in slope with heat flux for the oxidative steps. At the end of the test, the fiberglass had melted, leaving re-solidified glass in the crucible.

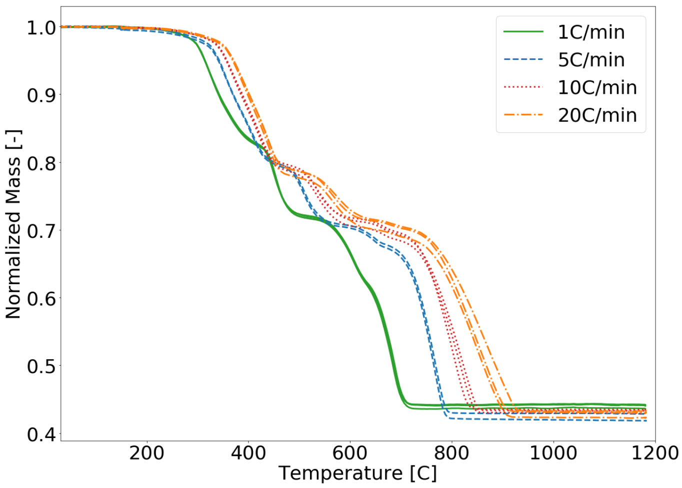

Figure 4-6. Normalized mass loss as a function of temperature for CFGFE at four heating rates decomposing in air. Pyrolysis reactions are fairly similar for different heating rates, while oxidation reactions occur at higher temperatures and slow rates for higher heating rates. Due to the presence of both CF and GF, CFGFE loses more mass than GFE but still has substantial mass remaining. 1 C/min has notably more remaining mass than the other heating rates; however, trends in remaining mass with higher heating rates are not evident.

4.4. Comparisons Between Composite Materials

As noted in the previous sections, the composites material share key characteristics during decomposition. In order to explore this further, we now present the same data, but rather than segregated by material, we will show all of the composite materials for a single heating rate.

4.4.1. Nitrogen

Figures 4-7 through 4-10 show the mass loss for the three composites, each at one of the four heating rates, in nitrogen. As the decomposition in nitrogen is driven by the pyrolysis of the epoxy, we can see there is little difference between the composites. We generally see that the fiberglass composite has the most residual mass, the carbon fiber the least, and the mixed composite lands between the two. This is because glass fiber is heavier, and thus is a larger percentage of the mass fraction, for the same volume fraction of epoxy.

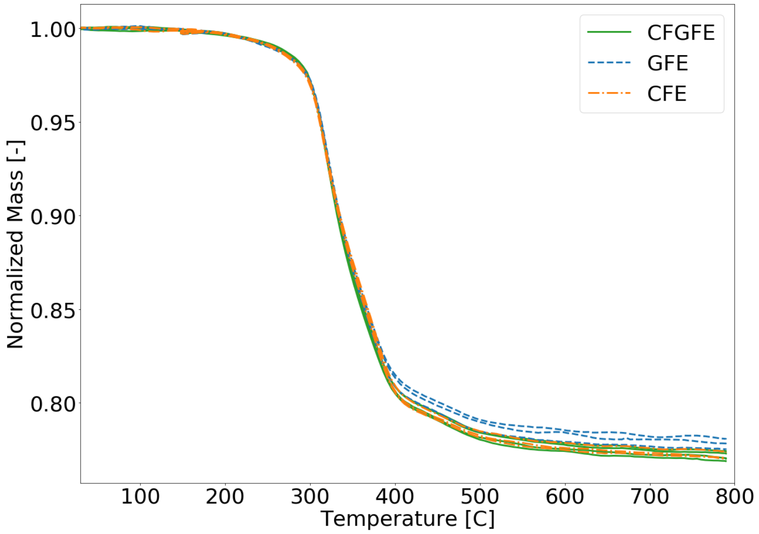

Figure 4-7. Normalized mass loss as a function of temperature for all composites (CFE, GFE, and CFGFE) in N_2 at 1 C/min. As anticipated, all three composites behave similarly in an inert environment, as the epoxy is responsible for all decomposition since the fibers do not decompose. Slight differences in remaining mass are likely due to slight differences in the percentage of epoxy between the three composites. Trends shown for this heating rate are consistent across heating rates.

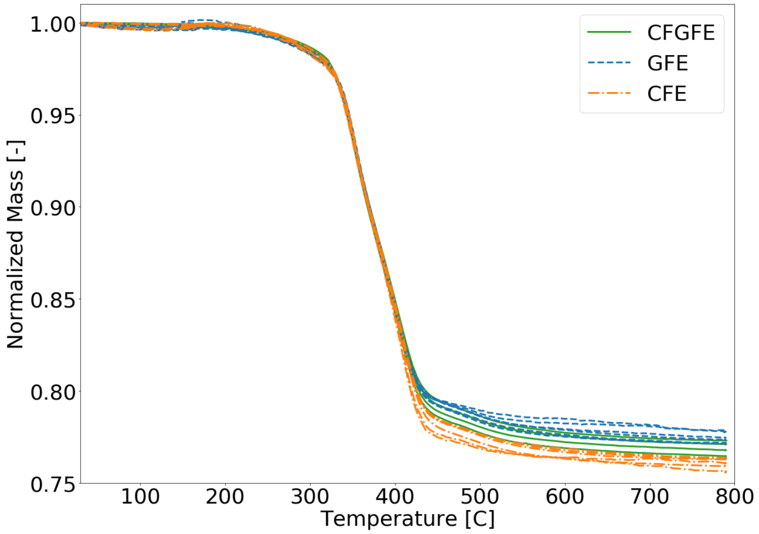

Figure 4-8. Normalized mass loss as a function of temperature for all composites (CFE, GFE, and CFGFE) in N_2 at 5 C/min. As anticipated, all three composites behave similarly in an inert environment, as the epoxy is responsible for all decomposition since the fibers do not decompose. Slight differences in remaining mass are likely due to slight differences in the percentage epoxy between the three composites. Trends shown for this heating rate are consistent across heating rates.

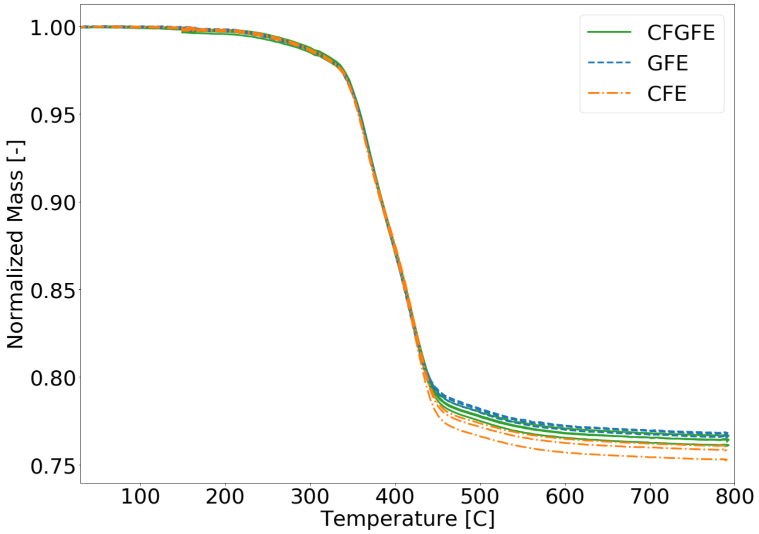

Figure 4-9. Normalized mass loss as a function of temperature for all composites (CFE, GFE, and CFGFE) in N_2 at 10 C/min. As anticipated, all three composites behave similarly in an inert environment, as the epoxy is responsible for all decomposition since the fibers do not decompose. Slight differences in remaining mass are likely due to slight differences in the percentage epoxy between the three composites. Trends shown for this heating rate are consistent across heating rates.

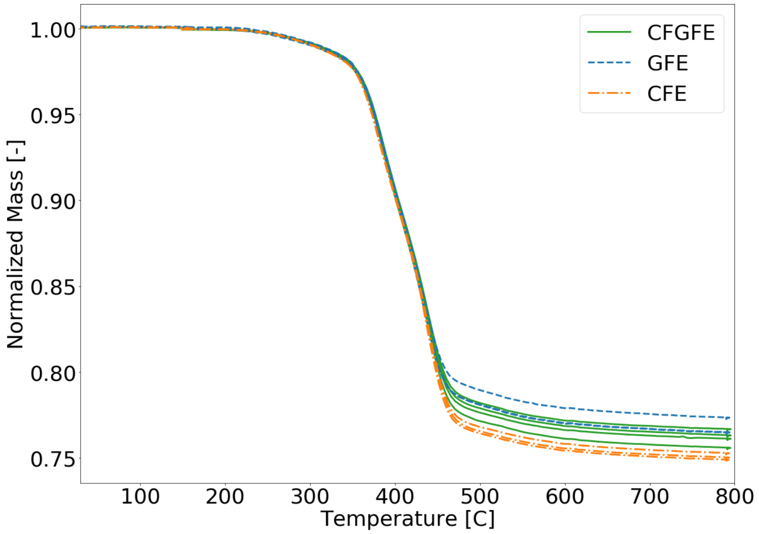

Figure 4-10. Normalized mass loss as a function of temperature for all composites (CFE, GFE, and CFGFE) in N_2 at 20 C/min. As anticipated, all three composites behave similarly in an inert environment, as the epoxy is responsible for all decomposition since the fibers do not decompose. Slight differences in remaining mass are likely due to slight differences in the percentage epoxy between the three composites. Trends shown for this heating rate are consistent across heating rates.

4.4.2. Air

Figures 4-11 through 4-14 shows the mass loss for all three composites in air. We can see that the initial mass loss (until ~70% of the mass remains) is very similar between the three composites. This is because this portion is driven by the pyrolysis of the epoxy, and the oxidation of the char formed from the epoxy pyrolysis. After this point, we see the fiberglass composite stop losing mass, as the glass is nearly inert. The carbon fiber composite continues to decompose, as the carbon oxides in air. The mixed composite also continues to decompose, but only to the mass fraction of fiberglass (~40%). While this curve at first appears fundamentally different from the carbon fiber curve, this is an illusion of the higher final mass. Both composites show changes in the mass loss curve at 650 C, 725 C, and stop loosing mass at 800 C.

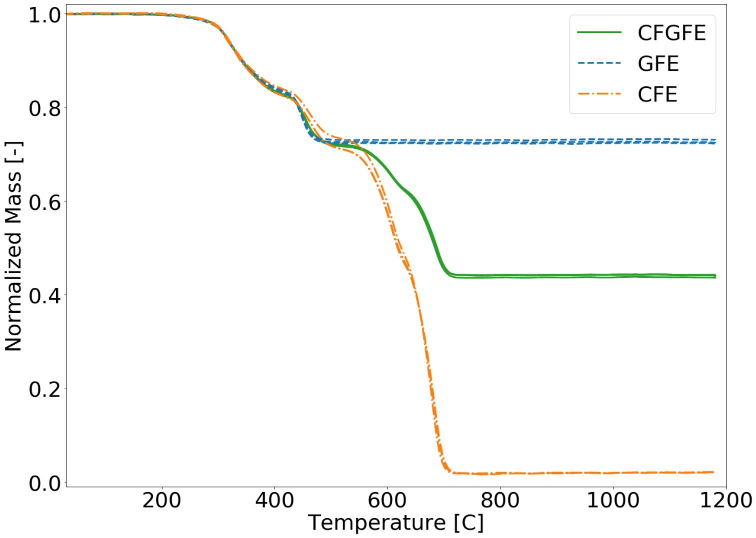

Figure 4-11. Normalized mass loss as a function of temperature for all composites (CFE, GFE, and CFGFE) in air at 1 C/min. The behavior of all three composites is similar at low temperatures (pyrolysis); however, two notables differences are clear in the oxidation reactions. First, the CFE and CFGFE exhibit additional reactions not seen in GFE around 600 C, due to the presence of carbon fiber. Second, the three composites have differing amounts of remaining mass. Decomposition here is related to the amount of epoxy and carbon fiber. The remaining mass seen for GFE and CFGFE is due to the presence of different amounts of GF in these two composites. Trends shown for this heating rate are consistent across heating rates.

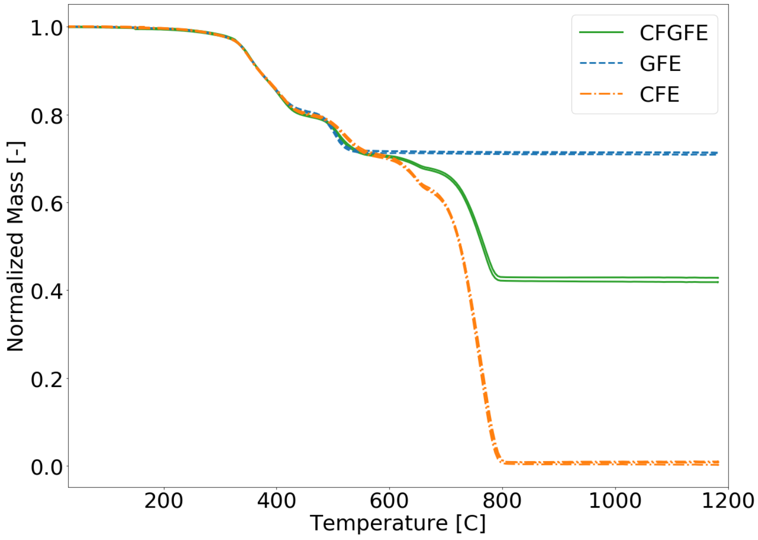

Figure 4-12. Normalized mass loss as a function of temperature for all composites (CFE, GFE, and CFGFE) in air at 5 C/min. The behavior of all three composites is similar at low temperatures (pyrolysis); however, two notables differences are clear in the oxidation reactions. First, the CFE and CFGFE exhibit additional reactions not seen in GFE around 700 C, due to the presence of carbon fiber. Second, the three composites have differing amounts of remaining mass. Decomposition here is related to the amount of epoxy and carbon fiber. The remaining mass seen for GFE and CFGFE is due to the presence of different amounts of GF in these two composites. Trends shown for this heating rate are consistent across heating rates.

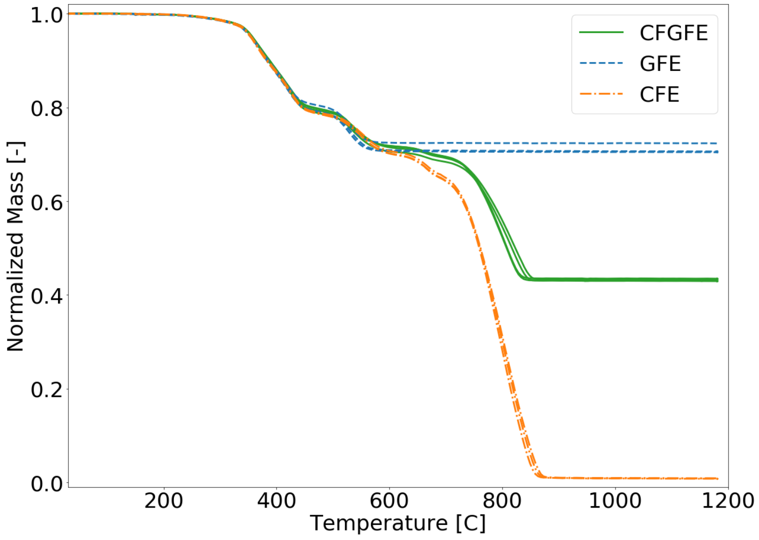

Figure 4-13. Normalized mass loss as a function of temperature for all composites (CFE, GFE, and CFGFE) in air at 10 C/min. The behavior of all three composites is similar at low temperatures (pyrolysis); however, two notables differences are clear in the oxidation reactions. First, the CFE and CFGFE exhibit additional reactions not seen in GFE around 700 C, due to the presence of carbon fiber. Second, the three composites have differing amounts of remaining mass. Decomposition here is related to the amount of epoxy and carbon fiber. The remaining mass seen for GFE and CFGFE is due to the presence of different amounts of GF in these two composites. Trends shown for this heating rate are consistent across heating rates.

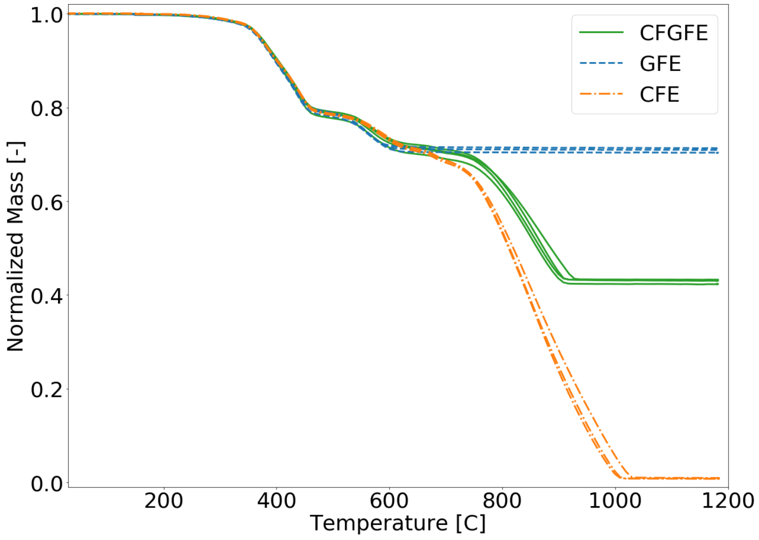

Figure 4-14. Normalized mass loss as a function of temperature for all composites (CFE, GFE, and CFGFE) in air at 20 C/min. The behavior of all three composites is similar at low temperatures (pyrolysis); however, two notables differences are clear in the oxidation reactions. First, the CFE and CFGFE exhibit additional reactions not seen in GFE around 700 C, due to the presence of carbon fiber. Second, the three composites have differing amounts of remaining mass. Decomposition here is related to the amount of epoxy and carbon fiber. The remaining mass seen for GFE and CFGFE is due to the presence of different amounts of GF in these two composites. Trends shown for this heating rate are consistent across heating rates.

5. PREDICTIONS OF COMPOSITE BEHAVIOR USING CONSTITUENTS

The presence of differing amounts of epoxy, glass fiber, and carbon fiber showed a clear influence on the differing decomposition behaviors of the composite materials in inert and oxidizing environments. To further understand this behavior, we investigate whether the superposition of the constituents in their respective mass fractions in a composite can be used to accurately describe the decomposition of the composite itself. The mass fractions of each constituent was determined using the product data sheets.

To create a prediction for a fiber-epoxy composite, the experimental mass loss versus temperature data for each constituent material is used, scaled by the mass fractions at which they occur in the initial composite, and summed at each temperature. To provide easier visual comparisons in the following figures, the data for the epoxy constituent is plotted after re-normalizing by its mass fraction in the composite and shifting to start at 1. Because the epoxy decomposes first, the superposed prediction based on constituents must match the shifted epoxy curve at low temperatures. Plotting the epoxy curved shifted in this way allows direct comparison of when the deviation from the prediction based on constituents occurs.

5.1. Carbon Fiber Epoxy Composite

5.1.1. CFE in Nitrogen

Figures 5-1 through 5-4 show the prediction for a carbon fiber epoxy composite, using the information from the carbon fiber and epoxy constituent data, for the four heating rates. In these plots, the black solid line represents the prediction. The prediction is then compared to the actual composite (blue dashes). Here we can see that the prediction tracks with the mass loss curve of the epoxy. This is unsurprising, as in nitrogen the mass loss of the composite is due to the pyrolysis of the epoxy. The epoxy alone lost ~2% to 4% more mass than the composite, and this number decreases with heating rate. This would indicate that the presence of the carbon fiber, as well as the faster heating rate, favor a reaction that creates more char. However, this small difference in the final mass does not eliminate the usefulness of this tool.

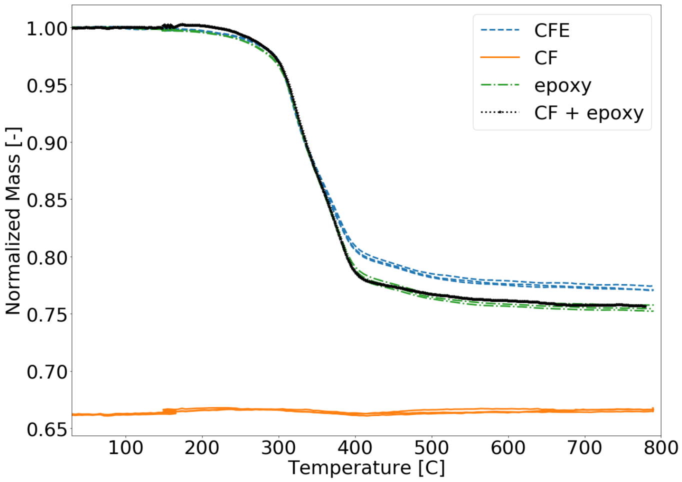

Figure 5-1. Normalized mass as a function of temperature for the decomposition of CFE and its constituents, epoxy and carbon fiber, in N_2 prediction at 1 C/min. The line indicating CF + epoxy shows the superposition of the constituents, which aligns with the epoxy mass loss curve, as anticipated. The prediction of CF + epoxy agrees fairly well with the actual CFE decomposition; however, CFE has more remaining mass at the end of the test.

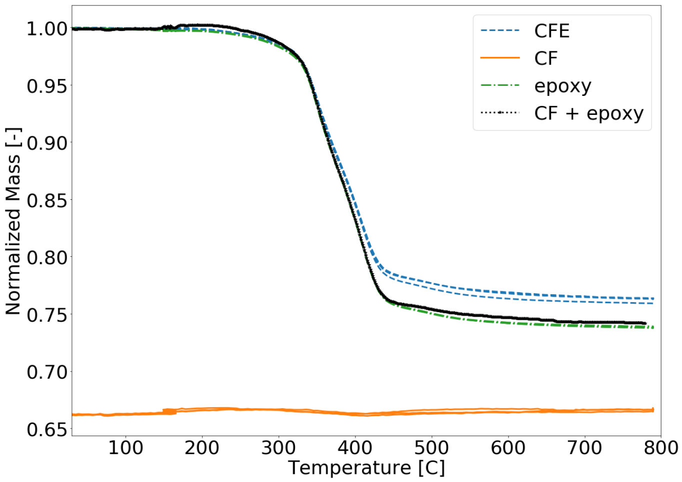

Figure 5-2. Normalized mass as a function of temperature for the decomposition of CFE and its constituents, epoxy and carbon fiber, in N_2 prediction at 5 C/min. The line indicating CF + epoxy shows the superposition of the constituents, which aligns with the epoxy mass loss curve, as anticipated. The prediction of CF + epoxy agrees fairly well with the actual CFE decomposition; however, CFE has more remaining mass at the end of the test.

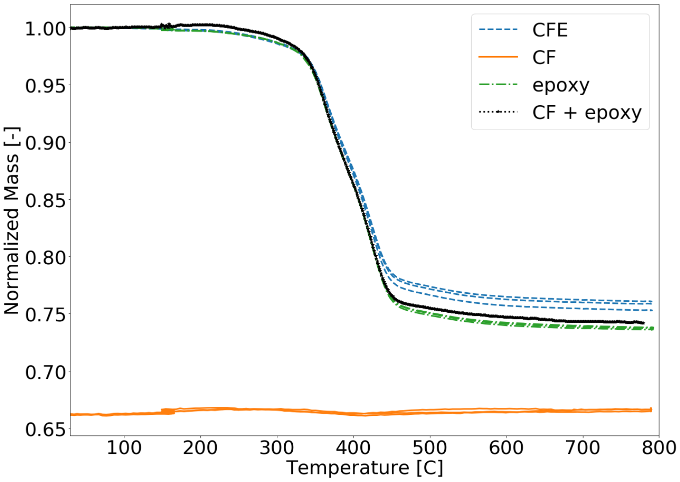

Figure 5-3. Normalized mass as a function of temperature for the decomposition of CFE and its constituents, epoxy and carbon fiber, in N_2 prediction at 10 C/min. The line indicating CF + epoxy shows the superposition of the constituents, which aligns with the epoxy mass loss curve, as anticipated. The prediction of CF + epoxy agrees fairly well with the actual CFE decomposition; however, CFE has more remaining mass at the end of the test.

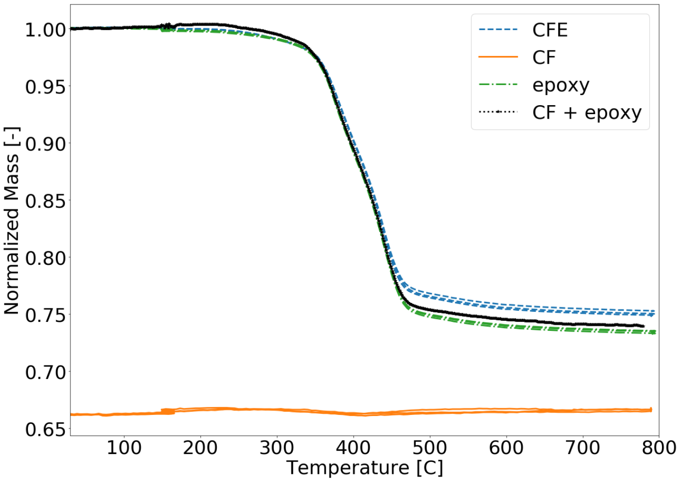

Figure 5-4. Normalized mass as a function of temperature for the decomposition of CFE and its constituents, epoxy and carbon fiber, in N_2 prediction at 20 C/min. The line indicating CF + epoxy shows the superposition of the constituents, which aligns with the epoxy mass loss curve, as anticipated. The prediction of CF + epoxy agrees fairly well with the actual CFE decomposition; however, CFE has more remaining mass at the end of the test.

5.1.2. CFE in Air

Figures 5-5 through 5-8 shows the results for predicting decomposition of the carbon fiber epoxy composite in air. We again see the prediction closely follows the mass loss curve of the epoxy, before switching over to the carbon fiber, around 600 C. As was the case in the nitrogen environment, the prediction is close to the actual material, but not exact. Here, particularly for the oxidizing reactions, we see a shift in temperature of when reactions being. In general, the prediction initiates the reactions at temperatures 50 C lower than the actual composite. However, as was the case in nitrogen, this result is promising when viewed through the lens of material design.

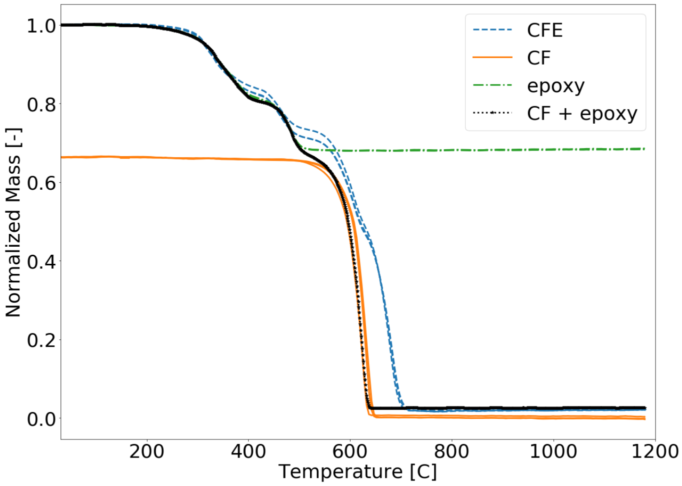

Figure 5-5. Normalized mass as a function of temperature for the decomposition of CFE and its constituents, epoxy and carbon fiber, in air prediction at 1 C/min. Here, epoxy and carbon fiber are scaled by their respective mass fractions in the composite. The constituents predict oxidation reactions happening at lower temperatures, but still capture the reaction rates. The prediction captures the remaining mass well.

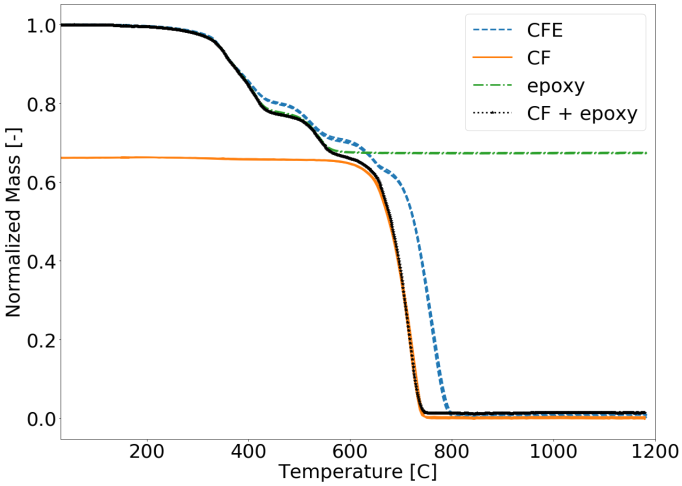

Figure 5-6. Normalized mass as a function of temperature for the decomposition of CFE and its constituents, epoxy and carbon fiber, in air prediction at 5 C/min. Here, epoxy and carbon fiber are scaled by their respective mass fractions in the composite. The constituents predict oxidation reactions happening at lower temperatures (approximately 50 C), but still capture the reaction rates. The prediction captures the remaining mass well.

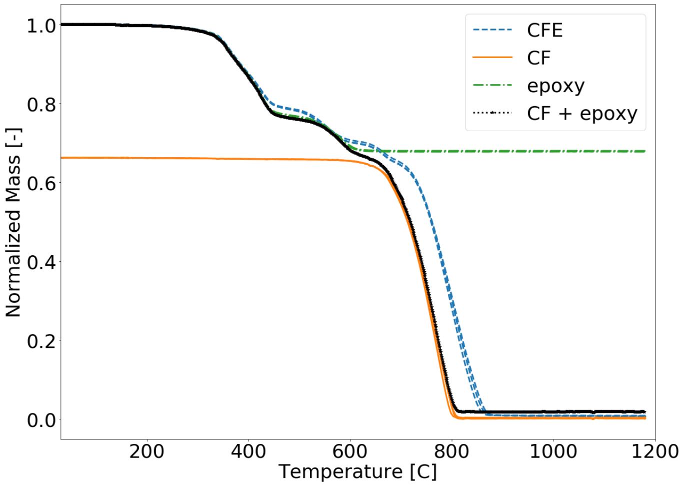

Figure 5-7. Normalized mass as a function of temperature for the decomposition of CFE and its constituents, epoxy and carbon fiber, in air prediction at 10 C/min. Here, epoxy and carbon fiber are scaled by their respective mass fractions in the composite. The constituents predict oxidation reactions happening at lower temperatures, but still capture the reaction rates. The prediction slightly overestimates the remaining mass.

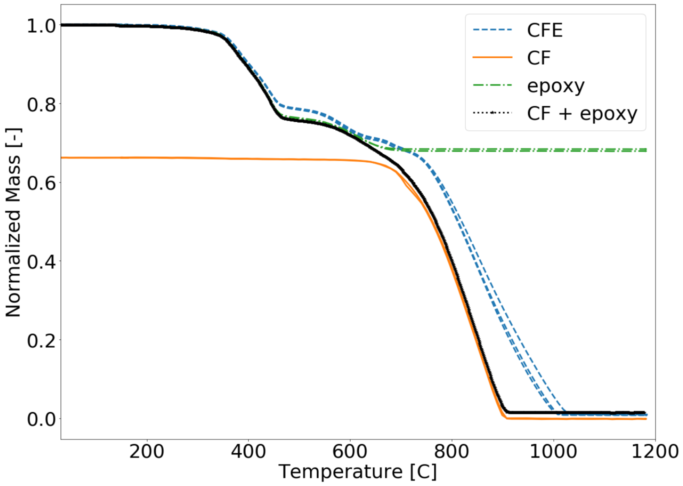

Figure 5-8. Normalized mass as a function of temperature for the decomposition of CFE and its constituents, epoxy and carbon fiber, in air prediction at 20 C/min. Here, epoxy and carbon fiber are scaled by their respective mass fractions in the composite. The constituents predict oxidation reactions happening at lower temperatures, but still capture the reaction rates. The prediction captures the remaining mass well.

5.2. Glass Fiber Epoxy Composite

5.2.1. GFE in Nitrogen

Figures 5-9 through 5-12 show the predictions for the fiberglass epoxy composite. As was the case with the carbon fiber composite, the prediction follows the mass loss of the epoxy. This is due to the glass being inert, and thus losing no mass. The final mass loss is again over predicted by 5%, which is consistent with the composite materials favoring a char forming reaction.

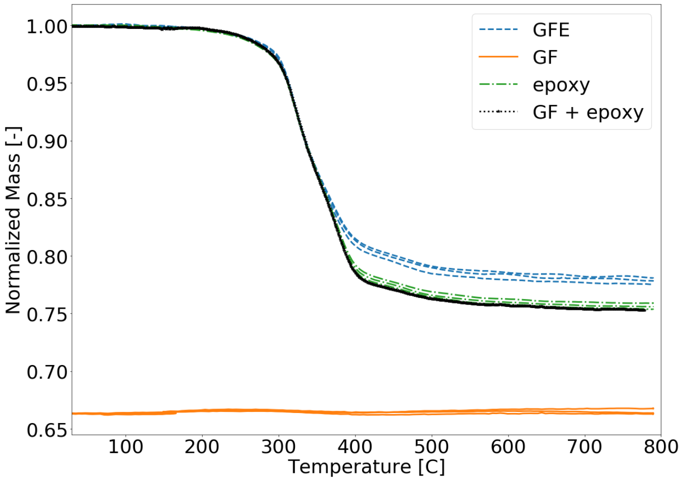

Figure 5-9. Normalized mass as a function of temperature for the decomposition of GFE and its constituents, epoxy and glass fiber, in N_2 prediction at 1 C/min. The line indicating GF + epoxy shows the superposition of the constituents, which aligns with the epoxy mass loss curve, as anticipated. The prediction of GF + epoxy agrees fairly well with the actual GFE decomposition; however, GFE has more remaining mass at the end of the test. This could be due to the glass fiber affecting heat transfer to the epoxy. Samples were left in layers, rather than ground, in case of impacts of structure on the decomposition.

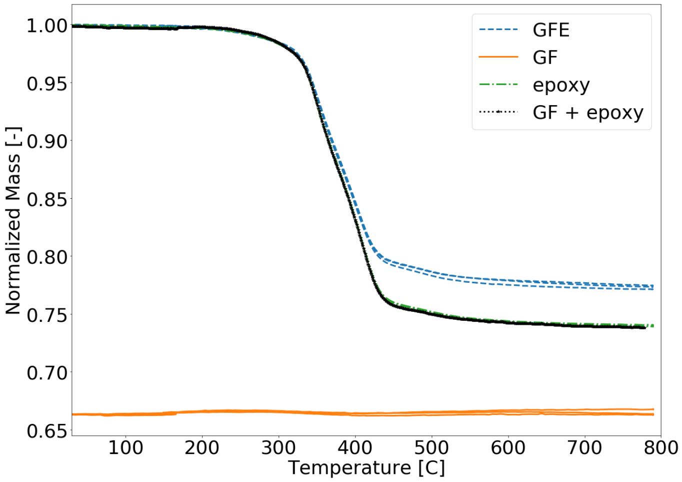

Figure 5-10. Normalized mass as a function of temperature for the decomposition of GFE and its constituents, epoxy and glass fiber, in N_2 prediction at 5 C/min. The line indicating GF + epoxy shows the superposition of the constituents, which aligns with the epoxy mass loss curve, as anticipated. The prediction of GF + epoxy agrees fairly well with the actual GFE decomposition; however, GFE has more remaining mass at the end of the test. This could be due to the glass fiber affecting heat transfer to the epoxy. Samples were left in layers, rather than ground, in case of impacts of structure on the decomposition.

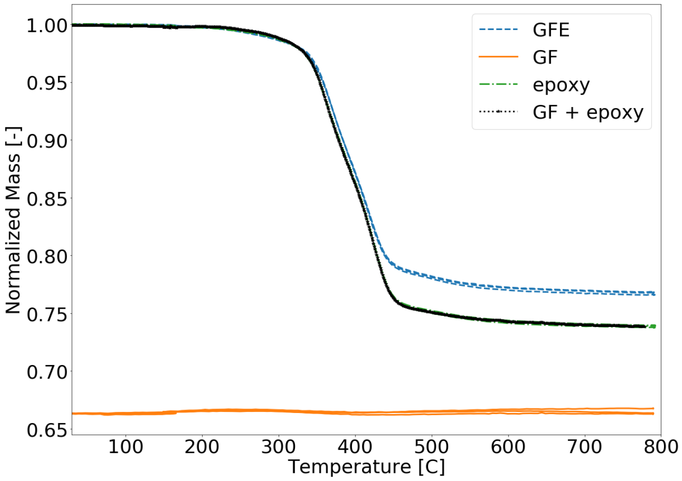

Figure 5-11. Normalized mass as a function of temperature for the decomposition of GFE and its constituents, epoxy and glass fiber, in N_2 prediction at 10 C/min. The line indicating GF + epoxy shows the superposition of the constituents, which aligns with the epoxy mass loss curve, as anticipated. The prediction of GF + epoxy agrees fairly well with the actual GFE decomposition; however, GFE has more remaining mass at the end of the test. This could be due to the glass fiber affecting heat transfer to the epoxy. Samples were left in layers, rather than ground, in case of impacts of structure on the decomposition.

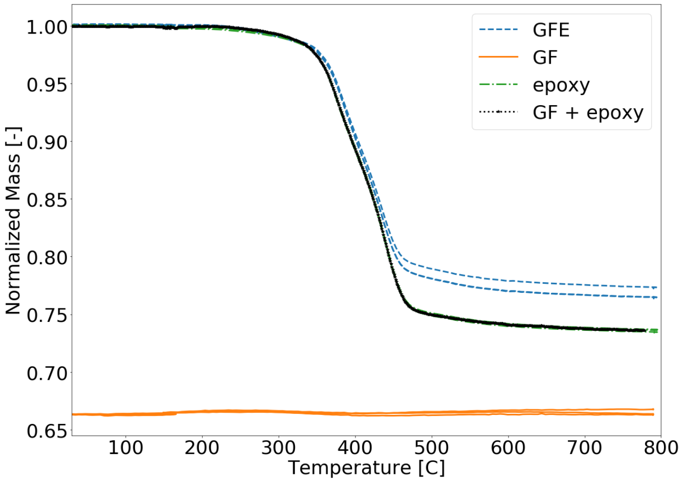

Figure 5-12. Normalized mass as a function of temperature for the decomposition of GFE and its constituents, epoxy and glass fiber, in N_2 prediction at 20 C/min. The line indicating GF + epoxy shows the superposition of the constituents, which aligns with the epoxy mass loss curve, as anticipated. The prediction of GF + epoxy agrees fairly well with the actual GFE decomposition; however, GFE has more remaining mass at the end of the test. This could be due to the glass fiber affecting heat transfer to the epoxy. Samples were left in layers, rather than ground, in case of impacts of structure on the decomposition.

5.2.2. GFE in Air

Figures 5-13 through 5-16 show the predictions for the fiberglass epoxy composite in air for all heating rates. Again, since the glass fiber is inert, the prediction tracks with the decomposition of epoxy. The final mass loss is over predicted by 3% to 5%, and there is also an increase in the onset temperature of the oxidizing reactions (those over 400 C). This again shows that the presence of the fibers does favor different reaction pathways than with the epoxy alone, however these results do still show promise for material design.

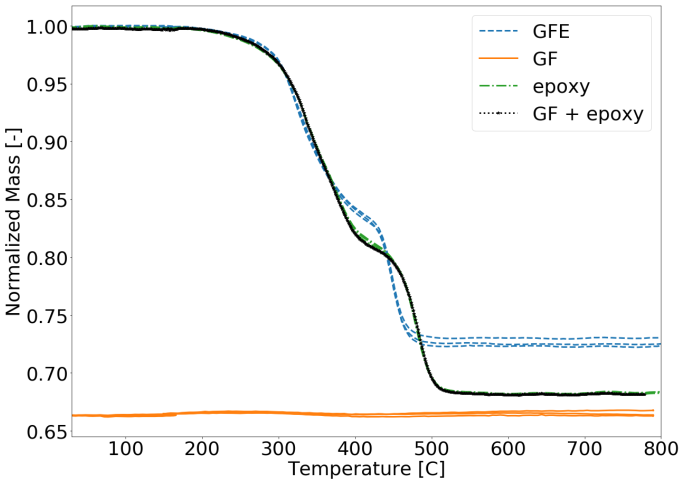

Figure 5-13. Normalized mass as a function of temperature for the decomposition of GFE and its constituents, epoxy and glass fiber, in air prediction at 1 C/min. Here, epoxy and glass fiber are scaled by their respective mass fractions in the composite. Glass fiber data is shown from N_2 tests because these fibers do not react. Therefore, the GFE decomposition is predicted by the behavior of the epoxy, similar to the predictions in an inert environment. Unlike for the CFE, the GF + epoxy predicts reactions at slightly higher temperatures. Here, the prediction underestimates the mass remaining by about 5%. These differences are assumed to be due to the same behaviors as the differences seen in the inert environment.

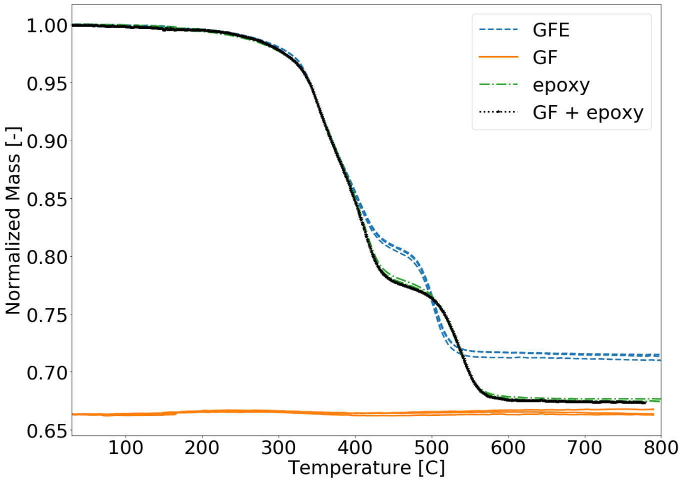

Figure 5-14. Normalized mass as a function of temperature for the decomposition of GFE and its constituents, epoxy and glass fiber, in air prediction at 5 C/min. Here, epoxy and glass fiber are scaled by their respective mass fractions in the composite. Glass fiber data is shown from N_2 tests because these fibers do not react. Therefore, the GFE decomposition is predicted by the behavior of the epoxy, similar to the predictions in an inert environment. Unlike for the CFE, the GF + epoxy predicts reactions at slightly higher temperatures. Here, the prediction underestimates the mass remaining by about 5%. These differences are assumed to be due to the same behaviors as the differences seen in the inert environment.

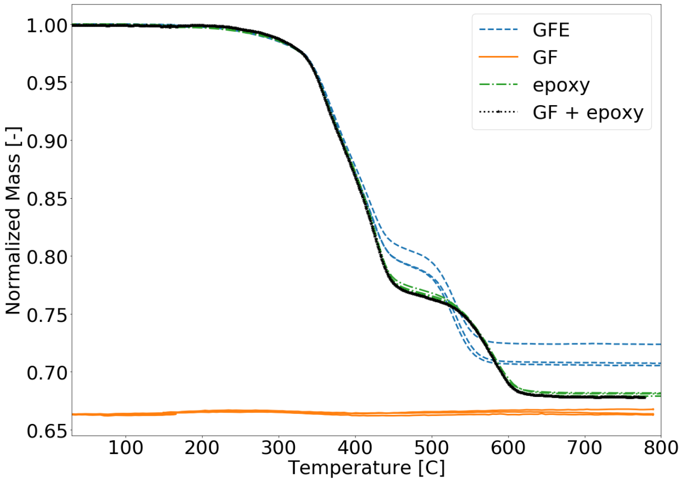

Figure 5-15. Normalized mass as a function of temperature for the decomposition of GFE and its constituents, epoxy and glass fiber, in air prediction at 10 C/min. Here, epoxy and glass fiber are scaled by their respective mass fractions in the composite. Glass fiber data is shown from N_2 tests because these fibers do not react. Therefore, the GFE decomposition is predicted by the behavior of the epoxy, similar to the predictions in an inert environment. Unlike for the CFE, the GF + epoxy predicts reactions at slightly higher temperatures. Here, the prediction underestimates the mass remaining by about 5%. These differences are assumed to be due to the same behaviors as the differences seen in the inert environment.

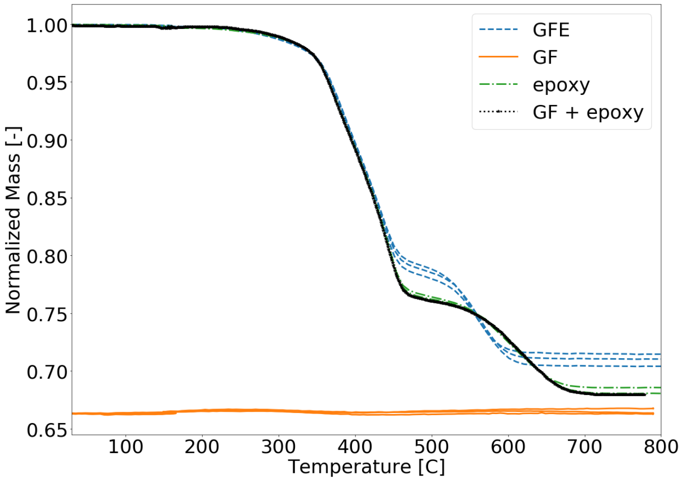

Figure 5-16. Normalized mass as a function of temperature for the decomposition of GFE and its constituents, epoxy and glass fiber, in air prediction at 20 C/min. Here, epoxy and glass fiber are scaled by their respective mass fractions in the composite. Glass fiber data is shown from N_2 tests because these fibers do not react. Therefore, the GFE decomposition is predicted by the behavior of the epoxy, similar to the predictions in an inert environment. Unlike for the CFE, the GF + epoxy predicts reactions at slightly higher temperatures. Here, the prediction underestimates the mass remaining by about 5%. These differences are assumed to be due to the same behaviors as the differences seen in the inert environment.

5.3. Combined Carbon Fiber-Glass Fiber Epoxy Composite

The this section the theory of being able to predict the mass loss curve of a designed material is put to the test. In designing a material, different combinations of materials may be desired, for example mixing fiberglass and carbon fiber in order achieve required mechanical properties. Here we attempt to predict the behavior of a mixed carbon fiber fiberglass epoxy composite.

5.3.1. CFGFE in Nitrogen

In Figures 5-17 through 5-20, the prediction for the mixed composite are presented for all heating rates. As we saw in the previous sections, the epoxy pyrolysis is the dominate source of decomposition in nitrogen, and for the mix composite we see the same result. Again, the prediction is about 5% less than the actual composite, though this difference in the residual mass is the main difference between the prediction and the actual material. Generally, this prediction would work well in a material design phase.

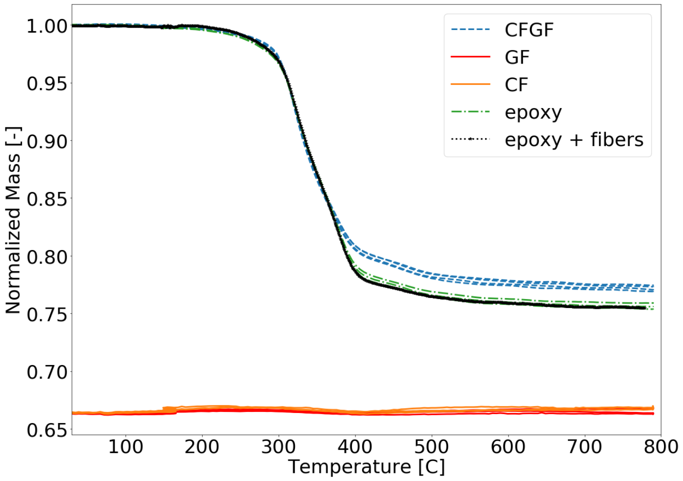

Figure 5-17. Normalized mass as a function of temperature for the decomposition of CFGFE and its constituents, epoxy, carbon fiber, and glass fiber, in N_2 at 1 C/min. The line indicating epoxy + fibers shows the superposition of the constituents, which aligns with the epoxy mass loss curve, as anticipated. The prediction of epoxy + fibers agrees fairly well with the actual CFGFE decomposition; however, CFGFE has more remaining mass at the end of the test. This could be due to the fibers affecting heat transfer to the epoxy. Samples were left in layers, rather than ground, in case of impacts of structure on the decomposition.

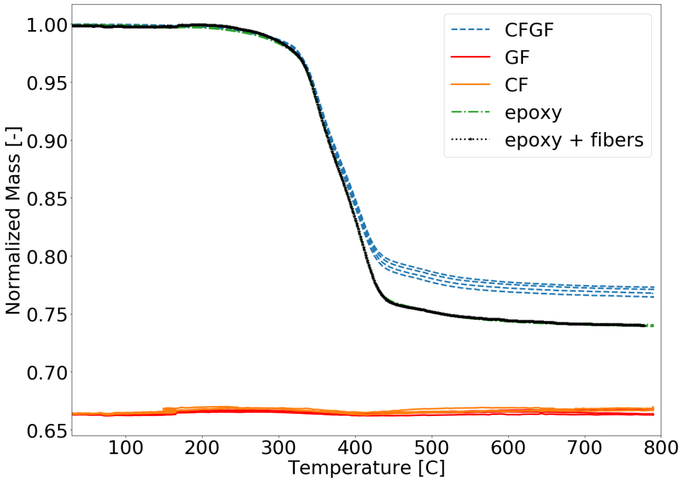

Figure 5-18. Normalized mass as a function of temperature for the decomposition of CFGFE and its constituents, epoxy, carbon fiber, and glass fiber, in N_2 at 5 C/min. The line indicating epoxy + fibers shows the superposition of the constituents, which aligns with the epoxy mass loss curve, as anticipated. The prediction of epoxy + fibers agrees fairly well with the actual CFGFE decomposition; however, CFGFE has more remaining mass at the end of the test. This could be due to the fibers affecting heat transfer to the epoxy. Samples were left in layers, rather than ground, in case of impacts of structure on the decomposition.

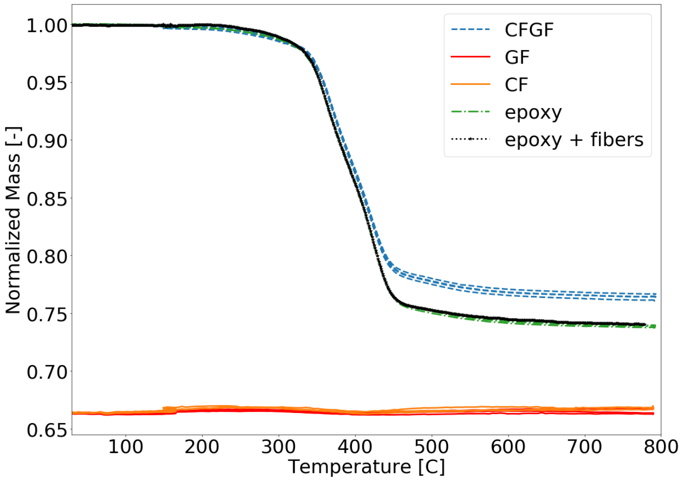

Figure 5-19. Normalized mass as a function of temperature for the decomposition of CFGFE and its constituents, epoxy, carbon fiber, and glass fiber, in N_2 at 10 C/min. The line indicating epoxy + fibers shows the superposition of the constituents, which aligns with the epoxy mass loss curve, as anticipated. The prediction of epoxy + fibers agrees fairly well with the actual CFGFE decomposition; however, CFGFE has more remaining mass at the end of the test. This could be due to the fibers affecting heat transfer to the epoxy. Samples were left in layers, rather than ground, in case of impacts of structure on the decomposition.

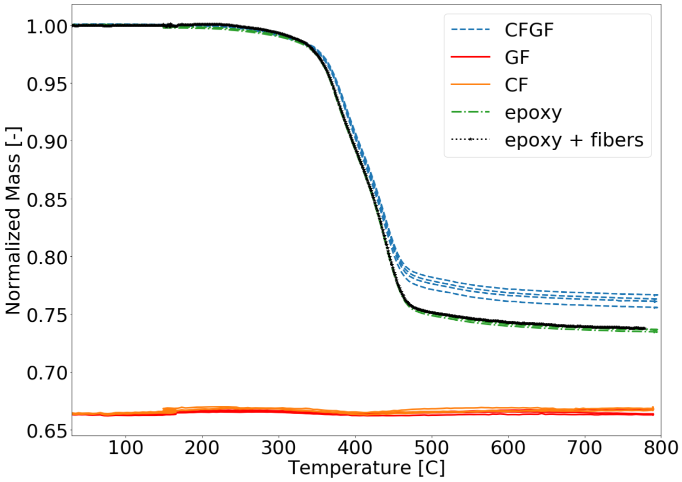

Figure 5-20. Normalized mass as a function of temperature for the decomposition of CFGFE and its constituents, epoxy, carbon fiber, and glass fiber, in N_2 at 20 C/min. The line indicating epoxy + fibers shows the superposition of the constituents, which aligns with the epoxy mass loss curve, as anticipated. The prediction of epoxy + fibers agrees fairly well with the actual CFGFE decomposition; however, CFGFE has more remaining mass at the end of the test. This could be due to the fibers affecting heat transfer to the epoxy. Samples were left in layers, rather than ground, in case of impacts of structure on the decomposition.

5.3.2. CFGFE in Air

Figures 5-21 through 5-24 show the results for the prediction of the mixed composite for all heating rates. The prediction tracks well with the actual material until the oxidizing reaction begin (around 450 C). At this point we see the prediction having a lower activation temperature than the actual material. The prediction improved as the heating rate increases, because the carbon fiber oxidation occurs over a wider range of temperatures than at the lower temperatures. Here was also see that the final mass is slightly over predicted, whereas for the cases it was under predicted. This is likely due to accuracy in defining the exact mass fraction of carbon fiber, fiberglass, and epoxy. However, these issues are minor, and the prediction does a good job of recreating the actual material.

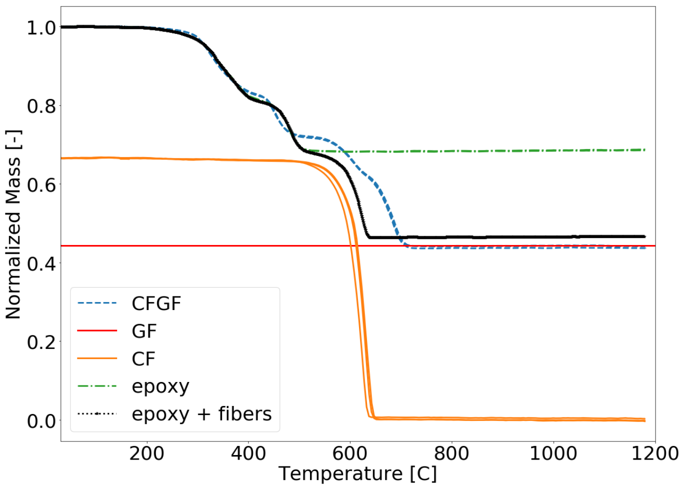

Figure 5-21. Normalized mass as a function of temperature for the decomposition of CFGFE and its constituents, epoxy, carbon fiber, and glass fiber, in air at 1 C/min. Here, epoxy and carbon fiber are scaled by their respective mass fractions in the composite. Glass fiber is plotted at its mass fraction, assuming no decomposition, but not plotted from experiments. The constituents predict oxidation reactions happening at lower temperatures with slightly different reaction rates for the late oxidation reactions (around 700 C). The prediction also slightly overestimates the remaining mass.

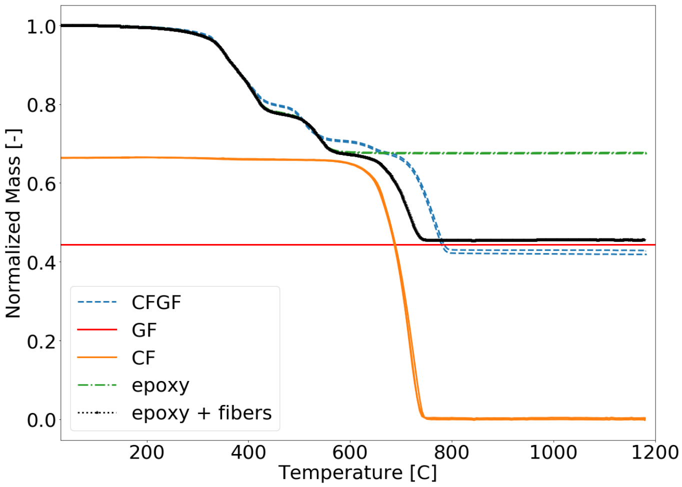

Figure 5-22. Normalized mass as a function of temperature for the decomposition of CFGFE and its constituents, epoxy, carbon fiber, and glass fiber, in air at 5 C/min. Here, epoxy and carbon fiber are scaled by their respective mass fractions in the composite. Glass fiber is plotted at its mass fraction, assuming no decomposition, but not plotted from experiments. The slight difference between the remaining mass of the CFGFE and the mass fraction of GFE is likely due to uncertainties in manufacturing and/or in initial mass of the sample before heating compared to at the first time step. The constituents predict oxidation reactions happening at lower temperatures, but capture reaction rates fairly well. The prediction also slightly overestimates the remaining mass.

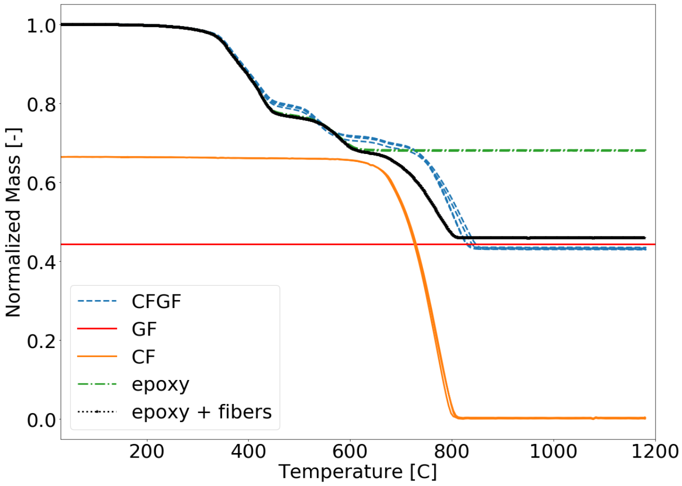

Figure 5-23. Normalized mass as a function of temperature for the decomposition of CFGFE and its constituents, epoxy, carbon fiber, and glass fiber, in air at 10 C/min. Here, epoxy and carbon fiber are scaled by their respective mass fractions in the composite. Glass fiber is plotted at its mass fraction, assuming no decomposition, but not plotted from experiments. The constituents predict oxidation reactions happening at lower temperatures with slightly different reaction rates for the late oxidation reactions (700-800 C). The prediction also slightly overestimates the remaining mass.

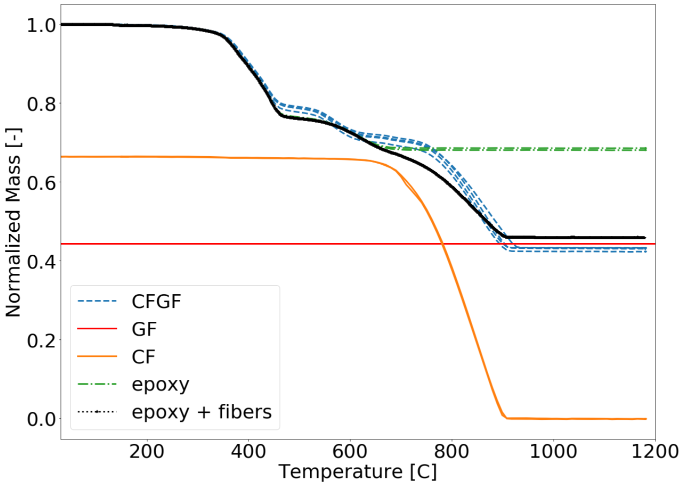

Figure 5-24. Normalized mass as a function of temperature for the decomposition of CFGFE and its constituents, epoxy, carbon fiber, and glass fiber, in air at 20 C/min. Here, epoxy and carbon fiber are scaled by their respective mass fractions in the composite. Glass fiber is plotted at its mass fraction, assuming no decomposition, but not plotted from experiments. The constituent prediction smooths out the final oxidation reactions in the 650-900 C range. The reason these reactions are not captured is currently unclear. The prediction also slightly overestimates the remaining mass.

6. SUMMARY AND FUTURE WORK

In this work we have presented the TGA data for the range of materials that make up a carbon and glass fiber composite: carbon fiber, glass fiber, epoxy, carbon fiber epoxy composite, glass fiber epoxy composite, and a mixed carbon fiber glass fiber epoxy composite. These materials were tested in both a nitrogen and dry air purge gas, at heating rates of 1, 5, 10, and 20 C/min, and mass loss vs temperature plots were presented to demonstrate how each material decomposed. We found for nitrogen environments, the pyrolysis of the epoxy was the driver for decomposition in all materials. Neither of the fibers decomposed in the nitrogen environment. In air, we found that the epoxy pyrolyzed, forming a char that could them oxidize. The carbon fiber also oxidized, meaning that for materials made from carbon fiber or epoxy (or the combination of the two), there was little material left at the end of the test. The inclusion of fiberglass, which is nearly inert, resulted in the final mass of decomposed samples being approximately equal to the mass of the fiberglass.

We then presented a methodology for predicting the decomposition behavior of composite materials, using the decomposition behavior of its constituents. We found that this methodology worked well for a first order approximation of the mixed material's decomposition, and therefore would be recommended for the material selection phase of a composite material. Combined with other property considerations, this provides a means to optimize a mixed glass and carbon fiber composite for various properties such as strength-to-weight, allowable strain, cost, and total energy released in an accident leading to a fire (where carbon fiber provides an additional fuel source compared to glass fiber). The mixing of the fibers with the epoxy does favor reactions that are not observed for the epoxy or carbon fiber alone, and therefore it will always be recommended to test the final material (or final candidates) to ensure the material behavior is within necessary parameters.

Future work will include creating decomposition mechanisms for each of these materials and composites. In addition, we will continue to explore the applicability of the prediction modeling, using the mechanisms generated to help guide and improve predictability. A possible approach is to combined the first-order superposition method presented here with a second-order refinement to try to capture the chemistry that is activated by combing the constituent materials.

Finally, tests on extracted glass fibers should be conducted in air to determine if the molten glass is forming oxides, which might help explain the observed mass increases in GFE above 800 C.

BIBLIOGRAPHY

[1] Takashi Ishikawa and Tsu Wei Chout. One-dimensional micromechanical analysis of woven fabric composites. *AIAA Journal*, 21(12):1714–1721, 1983. ISSN 00011452. doi: 10.2514/3.8314.

[2] P T Curtis and S M Bishop. An assessment of the potential of woven carbon fibre-reinforced plastics for high performance applications. 15(4):259–265, 1984. ISSN 00104361. doi: 10.1016/0010-4361(84)90706-7.

[3] James E. Brown, Emil Braun, and William H. Twilley. Cone Calorimeter Evaluation of the Flammability of Composite Materials. *Nsbir 88-3733*, (March), 1988.

[4] Jerome Paul Fanucci. Thermal Response of Radiantly Heated Kevlar and Graphite/Epoxy Composites. *Journal of Composite Materials*, 21(2):129–139, 1987. ISSN 1530793x. doi: 10.1177/002199838702100204.

[5] J. B. Henderson, J. A. Wiebelt, and M. R. Tant. A Model for the Thermal Response of Polymer Composite Materials with Experimental Verification. *Journal of Composite Materials*, 19(6): 579–595, 1985. ISSN 1530793X. doi: 10.1177/002199838501900608.

[6] J. B. Henderson and T. E. Wiecek. A Mathematical Model to Predict the Thermal Response of Decomposing, Expanding Polymer Composites. *Journal of Composite Materials*, 21(4): 373–393, 1987. ISSN 1530793x. doi: 10.1177/002199838702100406.

[7] CI Chang. The Effects on Polymer Composite Structures. *Theoretical and Applied Fracture Mechanics*, 6:113–120, 1986.

[8] W A Clayton. Constituent and Composite Thermal Conductivities Of Phenolic-Carbon A N D Phenolic-Graphite Ablators. In *AIAA / ASME 12th Strucutres, Structural Dynamics, and Materials Conference*, 1971. doi: 10.2514/6.1971-380. URL `http://arc.aiaa.org`.

[9] K. W. Garrett and H. M. Rosenberg. The thermal conductivity of epoxy-resin / powder composite materials. *Journal of Physics D: Applied Physics*, 7(9):1247–1258, 1974. ISSN 00223727. doi: 10.1088/0022-3727/7/9/311.

[10] J. B. Henderson, W. D. Emmerich, and E. Wassmer. Measurement of the specific heat and heat of decomposition of a polymer composite to high temperatures. *Journal of Thermal Analysis*, 33(4):1067–1077, 1988. ISSN 03684466. doi: 10.1007/BF01912731.

[11] D. Noël, J. J. Hechler, K. C. Cole, A. Chouliotis, and K. C. Overbury. Quantitative thermal characterization of carbon-epoxy composites using differential scanning calorimetry and thermogravimetric analysis. *Thermochimica Acta*, 125(C):191–208, mar 1988. ISSN 00406031. doi: 10.1016/0040-6031(88)87222-8.

[12] J. G. Quintiere, R. N. Walters, and S. Crowley. Flammability Properties of Aircraft Carbon-Fiber Structural Composite. Technical report, Federal Aviation Administration, DOT/FAA/AR-07/57, 2007.

[13] Parina Patel, T. Richard Hull, Richard E. Lyon, Stanislav I. Stoliarov, Richard N. Walters, Sean Crowley, and Natallia Safronava. Investigation of the thermal decomposition and flammability of PEEK and its carbon and glass-fibre composites. *Polymer Degradation and Stability*, 96(1): 12–22, jan 2011. ISSN 01413910. doi: 10.1016/j.polymdegradstab.2010.11.009.

[14] K. Chetehouna, N. Grange, N. Gascoin, L. Lemée, I. Reynaud, and S. Senave. Release and flammability evaluation of pyrolysis gases from carbon-based composite materials undergoing fire conditions. *Journal of Analytical and Applied Pyrolysis*, 134:136–142, sep 2018. ISSN 01652370. doi: 10.1016/j.jaap.2018.06.001.

[15] Alexander B. Morgan, Nicholas A. Gagliardi, William A. Price, and Mary L. Galaska. Cone calorimeter testing of S2 glass reinforced polymer composites. *Fire and Materials*, 33(7):323–344, nov 2009. ISSN 03080501. doi: 10.1002/fam.995. URL `http://doi.wiley.com/10.1002/fam.995`.

[16] Jianping Zhang, Michael A. Delichatsios, Talal Fateh, Mathieu Suzanne, and Sebastian Ukleja. Characterization of flammability and fire resistance of carbon fibre reinforced thermoset and thermoplastic composite materials. *Journal of Loss Prevention in the Process Industries*, 50:275–282, nov 2017. ISSN 0950-4230. doi: 10.1016/J.JLP.2017.10.004. URL `https://www.sciencedirect.com/science/article/pii/S095042301730880X`.

[17] T. Fateh, J. Zhang, M. Delichatsios, and T. Rogaume. Experimental investigation and numerical modelling of the fire performance for epoxy resin carbon fibre composites of variable thicknesses. *Fire and Materials*, 41(4):307–322, jun 2017. ISSN 03080501. doi: 10.1002/fam.2381. URL `http://doi.wiley.com/10.1002/fam.2381`.

[18] D. Quang Dao, J. Luche, F. Richard, T. Rogaume, C. Bourhy-Weber, and S. Ruban. Determination of characteristic parameters for the thermal decomposition of epoxy resin/carbon fibre composites in cone calorimeter. *International Journal of Hydrogen Energy*, 38(19): 8167–8178, jun 2013. ISSN 03603199. doi: 10.1016/j.ijhydene.2012.05.116.

[19] C. Di Blasi and I. S. Wichman. Effects of solid-phase properties on flames spreading over composite materials. *Combustion and Flame*, 102(3):229–240, 1995. ISSN 00102180. doi: 10.1016/0010-2180(95)00003-O.

[20] N. Régnier and S. Fontaine. Determination of the thermal degradation kinetic parameters of carbon fibre reinforced epoxy using TG. *Journal of Thermal Analysis and Calorimetry*, 64(2): 789–799, 2001. ISSN 14182874. doi: 10.1023/A:1011512932219.

[21] Pietro Tadini, Nathan Grange, Khaled Chetehouna, Nicolas Gascoin, Samuel Senave, and Isabelle Reynaud. Thermal degradation analysis of innovative PEKK-based carbon composites for high-temperature aeronautical components. *Aerospace Science and Technology*, 65:106–116, jun 2017. ISSN 1270-9638. doi: 10.1016/J.AST.2017.02.011. URL `https://www.sciencedirect.com/science/article/pii/S1270963816305740`.

[22] A.B. Dodd, B. Shelden, and K. L. Erickson. Numerical Simulation of Decomposition and Combustion of an Epoxy-Carbon-Fiber Composite. In *Interflam*, pages 407–412, Windsor, UK, 2013.

[23] Pauline Tranchard, Sophie Duquesne, Fabienne Samyn, Bruno Estèbe, and Serge Bourbigot. Kinetic analysis of the thermal decomposition of a carbon fibre-reinforced epoxy resin laminate. *Journal of Analytical and Applied Pyrolysis*, 126:14–21, jul 2017. ISSN 01652370. doi: 10.1016/j.jaap.2017.07.002.

[24] Mark B. McKinnon, Yan Ding, Stanislav I. Stoliarov, Sean Crowley, and Richard E. Lyon. Pyrolysis model for a carbon fiber/epoxy structural aerospace composite. *Journal of Fire Sciences*, 35(1):36–61, jan 2017. ISSN 15308049. doi: 10.1177/0734904116679422. URL `http://journals.sagepub.com/doi/10.1177/0734904116679422`.

[25] Carmen Branca, Colomba Di Blasi, Antonio Galgano, and Eva Milella. Thermal and kinetic characterization of a toughened epoxy resin reinforced with carbon fibers. *Thermochimica Acta*, 517(1-2):53–62, apr 2011. ISSN 00406031. doi: 10.1016/j.tca.2011.01.034.

[26] Valentin Biasi, Gillian Leplat, Frédéric Feyel, and Pierre Beauchêne. Heat and mass transfers within decomposing carbon fibers/epoxy resin composite materials. In *11th AIAA/ASME Joint Thermophysics and Heat Transfer Conference*, Atlanta, GA, 2014. doi: 10.2514/6.2014-2678. URL `http://arc.aiaa.org`.

[27] Chris Lautenberger and Carlos Fernandez-Pello. Generalized pyrolysis model for combustible solids. *Fire Safety Journal*, 44(6):819–839, 2009. ISSN 0379-7112. doi: 10.1016/j.firesaf.2009.03.011. URL `http://dx.doi.org/10.1016/j.firesaf.2009.03.011`.

APPENDIX A.

DISTRIBUTION

Email—Internal

Name	Org.	Sandia Email Address
CA Technical Library	8551	cateclib@sandia.gov

Hardcopy—Internal

Number of Copies	Name	Org.	Mailstop

Hardcopy—External

Number of Copies	Name(s)	Company Name and Company Mailing Address
1		

Sandia National Laboratories